

**MATHEMATICAL ENGINEERING
TECHNICAL REPORTS**

**Second-Order Cone Programming
with Warm Start for Elastoplastic Analysis
with von Mises Yield Criterion**

Kazuo YONEKURA and Yoshihiro KANNO

METR 2010-12

May 2010

DEPARTMENT OF MATHEMATICAL INFORMATICS
GRADUATE SCHOOL OF INFORMATION SCIENCE AND TECHNOLOGY
THE UNIVERSITY OF TOKYO
BUNKYO-KU, TOKYO 113-8656, JAPAN

WWW page: <http://www.keisu.t.u-tokyo.ac.jp/research/techrep/index.html>

The METR technical reports are published as a means to ensure timely dissemination of scholarly and technical work on a non-commercial basis. Copyright and all rights therein are maintained by the authors or by other copyright holders, notwithstanding that they have offered their works here electronically. It is understood that all persons copying this information will adhere to the terms and constraints invoked by each author's copyright. These works may not be reposted without the explicit permission of the copyright holder.

Second-Order Cone Programming with Warm Start for Elastoplastic Analysis with von Mises Yield Criterion

Kazuo Yonekura [†] and Yoshihiro Kanno [‡]

*Department of Mathematical Informatics,
University of Tokyo, Tokyo 113-8656, Japan*

Abstract

The incremental problem for quasistatic elastoplastic analysis with the von Mises yield criterion is treated within the framework of the second-order cone program (SOCP). We show that the classical flow rule under the von Mises yield criterion with the isotropic/kinematic hardening is equivalently written as a second-order cone complementarity problem. The minimization problems of the potential energy and the complementary energy for incremental analysis are then formulated as the primal-dual pair of SOCP problems, which are to be solved by using the primal-dual interior-point method. To enhance numerical performance in the course of tracing an equilibrium path, we propose a warm-start strategy for the interior-point method based on the primal-dual penalty method, in which the solution at the current loading step is found by solving a penalized SOCP problem from the initial point defined by using information of the solution at the previous loading step.

Keywords

Elastoplastic analysis; Interior-point method; Second-order cone programming; Warm-start strategy; von Mises yield criterion.

1 Introduction

This paper discusses a numerical algorithm with guaranteed convergence for the quasistatic analysis of elastoplastic structures, in which we solve a new formulation of the incremental problem based on the second-order cone programming (SOCP). We consider the von Mises yield criterion in conjunction with a combination of the linear isotropic and kinematic hardening laws. There is a vast literature on the numerical solutions of elastoplastic problems; among them, the radial return methods (or, the return-mapping algorithms) [31, 33, 34] are widely used nowadays. Although the convergence properties of the radial return methods are extensively studied [5, 7, 29, 38], theoretical guarantee of global convergence property to a solution is not still perfectly clear for incremental elastoplastic problems with hardening; see, [8, 18, 30], for related issues.

An alternative approach, which is also adopted in this paper, is to treat an elastoplastic problem as a mathematical programming problem. This approach was initiated by [9, 25, 26], with

[†]Present address: IHI Corporation, 3-1-1, Toyosu, Koto, Tokyo 135-8710, Japan.

[‡]Corresponding author. Address: Department of Mathematical Informatics, Graduate School of Information Science and Technology, University of Tokyo, Bunkyo, Tokyo 113-8656, Japan. E-mail: kanno@mist.i.u-tokyo.ac.jp. Phone: +81-3-5841-6906, Fax: +81-3-5841-6886.

employing a piecewise-linear approximation of the yield surface. Then the incremental problem is reduced to a convex quadratic problem. Subsequently, the optimization-based methods have been developed for more or less fine plasticity models, which include the augmented Lagrangian methods [10, 11], the parametric quadratic programming approaches [24, 42–44], the interior-point methods for general nonlinear programming problems [23], and the solution methods based on the linear complementarity problem [45], nonlinear complementarity problem [17, 36, 37], and so-called bi-potential formulation [16].

Recently, the Mohr–Coulomb criterion, which is often used in the limit analysis of geomaterials, has been shown to be represented by using the linear matrix inequality [6, 21]. Accordingly, the limit analysis problem can be reduced to a semidefinite programming (SDP) problem [22]. In contrast, in this paper we show that the von Mises criterion, which is conventionally used in the quasistatic analysis of metals, etc, can be represented by using several second-order cone constraints. Accordingly, the incremental problem for the quasistatic analysis is shown to be formulated as a minimization problem of the convex quadratic function over the second-order cone constraints, which is further reduced to an SOCP problem. Thus the issue of global convergence property of numerical solution for elastoplastic analysis is resolved particularly for the von Mises criterion; the solution of the incremental problem is guaranteed to be obtained by using the primal-dual interior-point method for SOCP; see, e.g. [1] for SOCP and the polynomial-time interior-point methods. A warm-start strategy for the interior-point method is also proposed in order to reduce the computational effort in the course of tracing an equilibrium path stepwise.

More specifically, in this paper we consider the associated flow rule in plasticity with the von Mises yield criterion. The effect of strain hardening is also incorporated by considering a combined law of the linear isotropic and kinematic hardening. In this setting we show that the evolution law in plasticity can be formulated as the so-called second-order cone complementarity (SOCC) conditions [15, 40], which have also been used to formulate the contact problem with the Coulomb friction [20].

In the course of the quasistatic analysis, the incremental problem is solved repeatedly by changing the boundary conditions stepwise and accordingly updating state variables. Therefore, in the proposed approach we solve a series of closely related SOCP problems. In such a situation, making use of the solution of the previous problem (or, more generally, some information obtained during the solution of the previous problem) for solving the subsequent problem is called *warm start* [2, 3, 12, 13, 19, 40]. If no such information is used for solving a new problem, we say that the current problem is solved from *cold start*. In this paper we discuss a warm-start strategy for the primal-dual interior-point method for SOCP.

Benson and Shanno [2] proposed a warm-start method for the primal-dual interior-point method solving the linear program (LP). As an extension of this method, we propose a warm-start strategy for the primal-dual interior-point method solving SOCP arising in the elastoplastic analysis. Recently, several special techniques of warm start have been proposed; see, e.g. [2, 13, 19] for the primal-dual interior-point methods solving LP, [3, 12] for the interior-point method solving general nonlinear programming problems, [27] for the dual interior-point method for SDP, and [40] for the Newton method solving SOCP.

This paper is organized as follows. Section 2 introduces the classical theory of associated

plasticity with the hardening law. In section 3, we show that the associated flow law with hardening can be reduced to SOCC conditions. Based on these SOCC conditions, in section 4 we formulate the minimization problems of the potential and complementary energies for the incremental problem as the the primal-dual pair of SOCP problems. To solve the presented SOCP formulation efficiently, a warm-start strategy for the primal-dual interior-point method is proposed in section 5. Numerical examples are shown in section 6: a plane-strain problem is solved in section 6.1, while a fully three-dimensional analysis is performed in section 6.2. Finally, conclusions are drawn in section 7.

We conclude this section by introducing our notation. All vectors are assumed to be column vectors. The $(m + n)$ dimension vector $(\mathbf{u}^T, \mathbf{v}^T)^T$ consisting of $\mathbf{u} \in \mathbb{R}^m$ and $\mathbf{v} \in \mathbb{R}^n$ is often written simply as (\mathbf{u}, \mathbf{v}) . We denote by \mathbb{R}_+^n the nonnegative orthant, i.e. $\mathbb{R}_+^n = \{\mathbf{v} = (v_i) \in \mathbb{R}^n \mid v_i \geq 0 \ (i = 1, \dots, n)\}$. By \mathcal{S} we denote the set of 3×3 real symmetric matrices. Since we always consider the Cartesian coordinate system, the distinction between the covariant and contravariant components of a tensor can be ignored. Accordingly, we write $\boldsymbol{\rho} \in \mathbb{R}^{3 \times 3}$ if $\boldsymbol{\rho}$ is a second-order tensor with the dimension three. Moreover, we write $\boldsymbol{\rho} \in \mathcal{S}$ if $\boldsymbol{\rho} \in \mathbb{R}^{3 \times 3}$ is symmetric. For any $\boldsymbol{\rho}, \boldsymbol{\tau} \in \mathbb{R}^{3 \times 3}$ we denote by $\boldsymbol{\rho} : \boldsymbol{\tau}$ their inner product, i.e. $\boldsymbol{\rho} : \boldsymbol{\tau} = \sum_{i=1}^3 \sum_{j=1}^3 \rho_{ij} \tau_{ij}$. The norm of $\boldsymbol{\rho}$, denoted $\|\boldsymbol{\rho}\|$, is then defined by $\|\boldsymbol{\rho}\| = \sqrt{\boldsymbol{\rho} : \boldsymbol{\rho}}$.

2 Plasticity with von Mises yield condition and linear hardening

This section preliminary introduces the classical theory of plasticity; see, e.g. [14, 31] for basic of plasticity theory. Specifically, we consider the associated flow rule based on the von Mises yield criterion and a combined law of isotropic/kinematic hardening. Throughout the paper we assume that the deformation is small.

For any tensor $\boldsymbol{\tau} \in \mathcal{S}$, we denote by $\dot{\boldsymbol{\tau}}$ the time derivative of $\boldsymbol{\tau}$. The deviator of $\boldsymbol{\tau} \in \mathcal{S}$, denoted $\text{dev}(\boldsymbol{\tau})$, is defined by

$$\text{dev}(\boldsymbol{\tau}) = \boldsymbol{\tau} - \frac{1}{3} \text{tr}(\boldsymbol{\tau}) \mathbf{I},$$

where $\mathbf{I} \in \mathcal{S}$ is the unit tensor. Let $\boldsymbol{\sigma} \in \mathcal{S}$ denote the stress tensor. Define $\boldsymbol{\eta} \in \mathcal{S}$ by

$$\boldsymbol{\eta} = \text{dev}(\boldsymbol{\sigma}) - \boldsymbol{\beta}, \tag{1}$$

where $\boldsymbol{\beta} \in \mathcal{S}$ is the back stress tensor which satisfies $\text{tr}(\boldsymbol{\beta}) = 0$. The von Mises yield function is given by

$$f(\boldsymbol{\sigma}, \alpha, \boldsymbol{\beta}) = \|\boldsymbol{\eta}\| - \sqrt{\frac{2}{3}} k_1(\alpha), \tag{2}$$

where $\alpha \geq 0$ is the internal hardening variable which represents the amount of plastic flow, and $k_1'(\alpha)$ is the isotropic hardening modulus. The admissible stress is then characterized by the inequality

$$f(\boldsymbol{\sigma}, \alpha, \boldsymbol{\beta}) \leq 0. \tag{3}$$

Let $\varepsilon_p \in \mathcal{S}$ denote the plastic strain. In a plastic loading state, say $\dot{\varepsilon}_p \neq \mathbf{o}$, the stress $\boldsymbol{\sigma}$ and the plastic strain rate $\dot{\varepsilon}_p$ should satisfy the associated flow rule

$$f(\boldsymbol{\sigma}, \alpha, \boldsymbol{\beta}) = 0, \quad (4)$$

$$\dot{\varepsilon}_p = \gamma \frac{\boldsymbol{\eta}}{\|\boldsymbol{\eta}\|}, \quad (5)$$

$$\gamma \geq 0, \quad (6)$$

where γ is called the consistency parameter, and we define $\mathbf{o}/\|\mathbf{o}\| = \mathbf{I}$ without loss of generality. The condition (5) means that $\dot{\varepsilon}_p$ is in the outer normal direction of the yield surface at $\boldsymbol{\sigma}$. We define the evolutions of α and $\boldsymbol{\beta}$ by

$$\dot{\alpha} = \sqrt{\frac{2}{3}}\gamma, \quad (7)$$

$$\dot{\boldsymbol{\beta}} = \frac{2}{3}k'_K(\alpha)\gamma \frac{\boldsymbol{\eta}}{\|\boldsymbol{\eta}\|}, \quad (8)$$

where $k'_K(\alpha)$ is the kinematic hardening modulus. From (5) and (7) we obtain $\dot{\alpha} = \sqrt{\frac{2}{3}}\|\dot{\varepsilon}_p\|$ to see that α corresponds to the conventional equivalent plastic strain. To see that $\text{tr}(\dot{\boldsymbol{\beta}}) = 0$ holds, we first observe from (1) that

$$\text{tr}(\dot{\boldsymbol{\eta}}) = \text{tr}(\text{dev}(\dot{\boldsymbol{\sigma}}) - \dot{\boldsymbol{\beta}}) = -\text{tr}(\dot{\boldsymbol{\beta}}) \quad (9)$$

is satisfied, because $\text{tr}(\text{dev}(\boldsymbol{\tau})) = 0$ for any $\boldsymbol{\tau} \in \mathcal{S}$. On the other hand, from (8) we obtain

$$\text{tr}(\dot{\boldsymbol{\beta}}) = \frac{2}{3\|\boldsymbol{\eta}\|}k'_K(\alpha)\gamma \text{tr}(\boldsymbol{\eta}). \quad (10)$$

Since $k'_K(\alpha)\gamma \geq 0$, (9) and (10) imply

$$\text{tr}(\dot{\boldsymbol{\beta}}) = \text{tr}(\boldsymbol{\eta}) = 0. \quad (11)$$

As a hardening law, we assume the combination of linear isotropic and kinematic hardening rules, which is defined by [31]

$$k'_I(\alpha) = \theta H, \quad (12)$$

$$k'_K(\alpha) = (1 - \theta)H, \quad (13)$$

where $H \geq 0$ and $\theta \in]0, 1[$ are constants. Note that θ represents the ratio of the effect of isotropic hardening with respect to the total strain hardening. It follows from (12) that the function k_I in (2) is written as

$$k_I(\alpha) = \sigma^Y + \theta H \alpha, \quad (14)$$

where $\sigma^Y > 0$ is a constant called the flow stress.

We next introduce the variables s_I and s_K by

$$s_I = \sqrt{\frac{2}{3}}\theta H \gamma, \quad (15)$$

$$s_K = \sqrt{\frac{2}{3}}(1 - \theta)H \gamma, \quad (16)$$

which represent the amounts of the isotropic and kinematic hardening effects, respectively. By using (15), the condition (3) together with (2) and (14) is rewritten as

$$\|\boldsymbol{\eta}\| - \sqrt{\frac{2}{3}}(\sigma^Y + s_I) \leq 0, \quad (17)$$

where α has been eliminated. On the other hand, by using (16), the condition (8) together with (13) is rewritten as

$$\dot{\boldsymbol{\beta}} = \sqrt{\frac{2}{3}} s_K \frac{\boldsymbol{\eta}}{\|\boldsymbol{\eta}\|}. \quad (18)$$

It follows from (5) that the consistency parameter γ is equal to the modulus of the plastic strain rate. Hence, the loading and unloading states are characterized as

$$\begin{aligned} \gamma > 0 & \Rightarrow f(\boldsymbol{\sigma}, \alpha, \boldsymbol{\beta}) = 0; & [\text{loading}] \\ f(\boldsymbol{\sigma}, \alpha, \boldsymbol{\beta}) < 0 & \Rightarrow \gamma = 0. & [\text{unloading}] \end{aligned}$$

This means that γ and $f(\boldsymbol{\sigma}, \alpha, \boldsymbol{\beta})$ satisfies the complementarity condition. By using the expression (17) of the yield condition, and from (6), we thus obtain

$$\gamma \geq 0, \quad (19a)$$

$$\|\boldsymbol{\eta}\| - \sqrt{\frac{2}{3}}(\sigma^Y + s_I) \leq 0, \quad (19b)$$

$$\gamma \left(\|\boldsymbol{\eta}\| - \sqrt{\frac{2}{3}}(\sigma^Y + s_I) \right) = 0. \quad (19c)$$

Consequently, the von Mises yield model with the linear hardening rule is represented by (1), (5), and (15)–(19).

3 Second-order cone complementarity formulations of plasticity law

The plasticity law introduced in section 2 is reduced to the form of second-order cone complementarity (SOCC) conditions.

3.1 Properties of the second-order cone complementarity condition

Usually, the second-order cone is defined by [1]

$$\{(x, \mathbf{z}) \in \mathbb{R} \times \mathbb{R}^n \mid x \geq \|\mathbf{z}\|\}, \quad (20)$$

where $\|\mathbf{z}\|$ is the standard Euclidean norm of the n -dimensional vector \mathbf{z} , i.e. $\|\mathbf{z}\| = \sqrt{\mathbf{z}^T \mathbf{z}}$. Thus the second-order cone (20) is the set of $(n + 1)$ -dimensional vectors. To treat the plasticity law, we here extend the notion of the second-order cone to the set

$$\{(x, \boldsymbol{\tau}) \in \mathbb{R} \times \mathbb{R}^{n \times n} \mid x \geq \|\boldsymbol{\tau}\|\}, \quad (21)$$

where $\|\boldsymbol{\tau}\|$ is the Frobenius norm of the $n \times n$ matrix (or, second-order tensors) $\boldsymbol{\tau}$, i.e. $\|\boldsymbol{\tau}\| = \sqrt{\boldsymbol{\tau} : \boldsymbol{\tau}}$. The complementarity condition over the second-order cone in (21) is then naturally defined as follows.

Definition 1. For $(x, \boldsymbol{\tau}), (y, \boldsymbol{\rho}) \in \mathbb{R} \times \mathbb{R}^{3 \times 3}$, by the second-order cone complementarity (SOCC) condition we mean

$$x \geq \|\boldsymbol{\tau}\|, \quad (22)$$

$$y \geq \|\boldsymbol{\rho}\|, \quad (23)$$

$$xy + \boldsymbol{\tau} : \boldsymbol{\rho} = 0. \quad (24)$$

■

The solution set of (22)–(24) is characterized as follows.

Proposition 2. $(x, \boldsymbol{\rho}) \in \mathbb{R} \times \mathbb{R}^{3 \times 3}$ and $(y, \boldsymbol{\tau}) \in \mathbb{R} \times \mathbb{R}^{3 \times 3}$ satisfy the SOCC condition if and only if any one of the following cases is true:

$$\text{Case 1: } x = 0, \boldsymbol{\rho} = \mathbf{o}, \quad y \geq \|\boldsymbol{\tau}\|; \quad (25a)$$

$$\text{Case 2: } x \geq \|\boldsymbol{\rho}\|, \quad y = 0, \boldsymbol{\tau} = \mathbf{o}; \quad (25b)$$

$$\text{Case 3: } xy \neq 0, \quad x = \|\boldsymbol{\rho}\|, \quad y = \|\boldsymbol{\tau}\|, \quad \boldsymbol{\tau} = -y \frac{\boldsymbol{\rho}}{\|\boldsymbol{\rho}\|}. \quad (25c)$$

Proof. Suppose that (22)–(24) are satisfied. If $x = 0$, then (22) implies $\boldsymbol{\tau} = \mathbf{o}$. Consequently, any $(y, \boldsymbol{\tau})$ satisfying (23) satisfies (24). This situation corresponds to Case 1. Similarly, if $y = 0$, then Case 2 becomes true. Conversely, it is easily seen that if either (25a) or (25b) holds, then (22)–(24) are satisfied.

We next consider the case of $xy \neq 0$, where (22)–(24) are supposed to be satisfied. Divide the both hand-sides of (24) by xy to obtain

$$\frac{\boldsymbol{\tau}}{x} : \left(-\frac{\boldsymbol{\rho}}{y} \right) = 1 \quad (26)$$

On the other hand, from (22) and (23) we obtain

$$\left\| \frac{\boldsymbol{\tau}}{x} \right\| \leq 1, \quad \left\| -\frac{\boldsymbol{\rho}}{y} \right\| \leq 1. \quad (27)$$

Application of the Cauchy–Schwarz inequality to (27) results in

$$\frac{\boldsymbol{\tau}}{x} : \left(-\frac{\boldsymbol{\rho}}{y} \right) \leq 1.$$

Moreover, we see that (26) holds if and only if there exists a $\lambda > 0$ satisfying

$$\frac{\boldsymbol{\tau}}{x} = \lambda \left(-\frac{\boldsymbol{\rho}}{y} \right), \quad \left\| \frac{\boldsymbol{\tau}}{x} \right\| = 1, \quad \left\| -\frac{\boldsymbol{\rho}}{y} \right\| = 1,$$

which coincides with Case 3. Conversely, it is immediate to see that (25c) implies (22)–(24). □

Among the three cases of Proposition 2, Case 3 in (25c) is particularly important, which means that $\boldsymbol{\tau}$ is in parallel with $-\boldsymbol{\rho}$. Our essential idea to obtain SOCC formulations for the elastoplastic problem is to make use of this property of the SOCC condition to express the conditions (5) and (18), which are dealt with in detail in sections 3.2 and 3.3, respectively.

3.2 Reformulation of flow law with isotropic hardening rule

The flow rule (5) and the yield condition (19), in the presence of the isotropic hardening, are reduced to an SOCC condition as follows.

Proposition 3. *Suppose that s_I and γ satisfy (15). Then $(s_I, \boldsymbol{\eta}) \in \mathbb{R} \times \mathcal{S}$ and $(\gamma, \dot{\boldsymbol{\epsilon}}_p) \in \mathbb{R} \times \mathcal{S}$ satisfy (5) and (19) if and only if $(\sqrt{\frac{2}{3}}(\sigma^Y + s_I), \boldsymbol{\eta})$ and $(\gamma, -\dot{\boldsymbol{\epsilon}}_p)$ satisfy SOCC condition, i.e.*

$$\sqrt{\frac{2}{3}}(\sigma^Y + s_I) \geq \|\boldsymbol{\eta}\|, \quad (28)$$

$$\gamma \geq \|\dot{\boldsymbol{\epsilon}}_p\|, \quad (29)$$

$$\sqrt{\frac{2}{3}}(\sigma^Y + s_I)\gamma - \boldsymbol{\eta} : \dot{\boldsymbol{\epsilon}}_p = 0. \quad (30)$$

Proof. Suppose that (28)–(30) are satisfied. It follows from Proposition 2 that $(\sqrt{2/3}(\sigma^Y + s_I), \boldsymbol{\eta})$ and $(\gamma, -\dot{\boldsymbol{\epsilon}}_p)$ satisfy (28)–(30) if and only if any one of the following conditions holds:

$$\text{Case 1: } \sqrt{\frac{2}{3}}(\sigma^Y + s_I) = 0, \quad \boldsymbol{\eta} = \mathbf{o}, \quad \gamma \geq \|\dot{\boldsymbol{\epsilon}}_p\|;$$

$$\text{Case 2: } \sqrt{\frac{2}{3}}(\sigma^Y + s_I) \geq \|\boldsymbol{\eta}\|, \quad \gamma = 0, \quad \dot{\boldsymbol{\epsilon}}_p = \mathbf{o};$$

$$\text{Case 3: } \sqrt{\frac{2}{3}}(\sigma^Y + s_I) = \|\boldsymbol{\eta}\|, \quad \gamma = \|\dot{\boldsymbol{\epsilon}}_p\|, \quad -\dot{\boldsymbol{\epsilon}}_p = -\gamma \frac{\boldsymbol{\eta}}{\|\boldsymbol{\eta}\|}$$

$$\text{where } \sqrt{\frac{2}{3}}(\sigma^Y + s_I)\gamma \neq 0.$$

Recall that $\sigma^Y > 0$ is a constant. Moreover, (29) implies $\gamma \geq 0$, from which and (15) we obtain $s_I \geq 0$. Therefore, $\sqrt{\frac{2}{3}}(\sigma^Y + s_I) > 0$, and hence Case 1 never happens. In Case 2, which corresponds to the unloading state, it is easy to see that (5) and (19) are satisfied. In Case 3, we firstly see that (5) is satisfied by equality. Moreover, substitution $\dot{\boldsymbol{\epsilon}}_p = \frac{\gamma}{\|\boldsymbol{\eta}\|}\boldsymbol{\eta}$ into (30) results in (19c). Consequently, (28)–(30) imply (5) and (19).

Conversely, suppose that (5) and (19) hold. Since (28) is identical to (19b), it suffices to show that (29) and (30) are satisfied. By taking the norms of the both hand-sides of (5), we obtain $\|\dot{\boldsymbol{\epsilon}}_p\| = \gamma$, and hence (29) is satisfied. By substituting (5), the left-hand side of (30) is reduced to

$$\begin{aligned} \sqrt{\frac{2}{3}}(\sigma^Y + s_I)\gamma - \boldsymbol{\eta} : \dot{\boldsymbol{\epsilon}}_p &= \sqrt{\frac{2}{3}}(\sigma^Y + s_I)\gamma - \boldsymbol{\eta} : \frac{\boldsymbol{\eta}}{\|\boldsymbol{\eta}\|}\gamma \\ &= \sqrt{\frac{2}{3}}(\sigma^Y + s_I)\gamma - \|\boldsymbol{\eta}\|\gamma. \end{aligned} \quad (31)$$

If $\gamma = 0$, (31) results in 0, and hence (30) is satisfied. If $\gamma \neq 0$, then (19c) implies

$$\|\boldsymbol{\eta}\| = \sqrt{\frac{2}{3}}(\sigma^Y + s_I).$$

Substitution of this relation into (31) shows that (30) is satisfied, which concludes the proof. \square

Compared with the traditional formulation of the flow rule, say (5) and (19), the SOCC formulation provided in Proposition 3 can be distinguished from the following aspects: the static variables $(s_I, \boldsymbol{\eta}) \in \mathbb{R} \times \mathcal{S}$ and kinematic variables $(\gamma, \dot{\boldsymbol{\epsilon}}_p) \in \mathbb{R} \times \mathcal{S}$ are subjected to the inequalities in the same form as seen in (28) and (29), while in (19a) and (19b) only γ is involved as a kinematic variable; the constraint condition (5) on the directions of $\dot{\boldsymbol{\epsilon}}_p$ and $\boldsymbol{\eta}$ does not appear explicitly in (28)–(30), although it is guaranteed to be satisfied at the solution. These properties play a key role to formulate the incremental problems in elastoplastic analysis as an SOCP problem in section 4.

3.3 Reformulation of kinematic hardening rule

Concerning the kinematic hardening, we show that the evolution rule of the back stress $\boldsymbol{\beta}$ can be represented as an SOCC condition as follows.

Proposition 4. *Suppose that γ , $\boldsymbol{\eta}$, and $\dot{\boldsymbol{\epsilon}}_p$ satisfy (5), and that γ and s_K satisfy (16). Then $s_K \in \mathbb{R}$, $\dot{\boldsymbol{\beta}} \in \mathcal{S}$, and $\boldsymbol{\eta} \in \mathcal{S}$ satisfy (18) if and only if $(\sqrt{\frac{2}{3}}s_K, \dot{\boldsymbol{\beta}})$ and $(\gamma, -\dot{\boldsymbol{\epsilon}}_p)$ satisfy the SOCC condition, i.e.*

$$\sqrt{\frac{2}{3}}s_K \geq \|\dot{\boldsymbol{\beta}}\|, \quad (32)$$

$$\gamma \geq \|\dot{\boldsymbol{\epsilon}}_p\|, \quad (33)$$

$$\sqrt{\frac{2}{3}}s_K\gamma - \dot{\boldsymbol{\beta}} : \dot{\boldsymbol{\epsilon}}_p = 0. \quad (34)$$

A proof of Proposition 4, which is based on Proposition 2 in a manner similar to Proposition 3, is given in appendix A.

The kinematic hardening rule (18), together with (5), requires that the rate of back stress $\dot{\boldsymbol{\beta}}$ should be in parallel with the plastic strain rate $\dot{\boldsymbol{\epsilon}}_p$. Proposition 4 asserts that this condition can be represented as the SOCC condition.

4 Second-order cone programming formulations of incremental problem

The incremental problem for quasistatic analysis of elastoplastic bodies is shown to be formulated as a primal-dual pair of SOCP (second-order cone programming) problems.

4.1 Incremental problem

We solve the incremental problems for quasistatic analysis of elastoplastic bodies by applying a standard spatial discretization based on the conventional finite element approximation. Hence, hereinafter we formulate the incremental problem and equivalent optimization problems for a finitely discretized elastoplastic structure.

Suppose that the domain Ω of the continuous solid is subdivided into the n^E finite elements. The weak form contributions are integrated within each finite element according to the standard finite element procedure. As usual, we employ the Gauss integration, and we denote by n^G the number of total Gauss evaluation points for the quadrature. The stress and strain tensors are evaluated at each Gauss point $q = 1, \dots, n^G$, and accordingly the constraint conditions, such as the yield criteria, are to be imposed at each Gauss point. For simplifying the notation, with the subscript “ q ” we denote the values of the strain and stress variables at the q th Gauss point, while by those variables without “ q ” we mean the assembled tensors for all $q = 1, \dots, n^G$; for example, we denote by $\boldsymbol{\varepsilon}_{pq}$ the plastic strain tensor at the p th Gauss point, while $\boldsymbol{\varepsilon}_p$ is the assemblage of $\boldsymbol{\varepsilon}_{p1}, \dots, \boldsymbol{\varepsilon}_{pn^G}$.

Let $\mathbf{u} \in \mathbb{R}^d$ and $\mathbf{t} \in \mathbb{R}^d$ denote the generalized nodal displacements and stresses, respectively, where d is the number of degrees of freedom. The set of indices of the degrees of freedom,

say $\{1, \dots, d\}$, is partitioned into two disjoint subsets as $J_u \cup J_t$, where the displacement u_j is prescribed to be \bar{u}_j for any $j \in J_u$ while the generalized nodal stress t_j is specified as \bar{t}_j for $j \in J_t$.

We denote by B^* the discrete equilibrium operator, so that the force-balance equation is given by

$$B^* \cdot \boldsymbol{\sigma} = \mathbf{t}, \quad (35)$$

where $\boldsymbol{\sigma}$ is the assemblage of $\boldsymbol{\sigma}_1, \dots, \boldsymbol{\sigma}_{n_G}$, as mentioned above. The discrete strain–displacement relation is then written as

$$\boldsymbol{\varepsilon} = B\mathbf{u}, \quad (36)$$

where B is the conjugate operator of B^* , which satisfies $\langle B^* \cdot \boldsymbol{\sigma}, \mathbf{u} \rangle = \langle \boldsymbol{\sigma}, B\mathbf{u} \rangle$ for any \mathbf{u} and $\boldsymbol{\sigma}$. Let $\boldsymbol{\varepsilon}_{eq} \in \mathcal{S}$ denote the elastic strain tensor. We denote by C_q the (forth-order) elasticity tensor. Then the constitutive law is given by

$$\boldsymbol{\sigma} = C : \boldsymbol{\varepsilon}_e. \quad (37)$$

Among the time interval $[0, T]$ under consideration, consider a specific subinterval $[\tau_0, \tau_1]$. The incremental problem is formulated as a quasistatic problem with respect to the unknown variables at time τ_1 when the variables at time τ_0 are known. With the superscript “0” we represent the values at time τ_0 , e.g. \mathbf{u}^0 for the displacement, and with (\cdot) the increments between τ_0 and τ_1 , e.g. $\dot{\mathbf{u}}$ for the incremental displacement. As exceptions, however, we represent by γ , s_I , and s_K the incremental values, because by definitions they are related to the plastic strain rate as seen in (5), (15), and (16). Moreover, concerning $\boldsymbol{\eta}$ defined by (1), we treat its total value at time τ_1 as a variable for convenience.

We are now in position to formulate the incremental problem. The force-balance equation, compatibility condition, and elastic constitutive law are given by (35), (36), and (37). It should be clear that the strain in (36) is additively decomposed to the elastic and plastic parts as $\boldsymbol{\varepsilon} = \boldsymbol{\varepsilon}_e + \boldsymbol{\varepsilon}_p$. The basic equations of the plasticity has been introduced section 2 as (1), (5), and (15)–(19). In order to simplify the notation, define $R_q^0 > 0$ by

$$R_q^0 = \sigma_q^Y + \int_0^{\tau_0} s_{Iq},$$

which represents the radius of the yield surface at τ_0 . Accordingly, the incremental problem for

the elastoplastic analysis is formulated as

$$\boldsymbol{\sigma}^0 + \dot{\boldsymbol{\sigma}} = C : (\boldsymbol{\varepsilon}_e^0 + \dot{\boldsymbol{\varepsilon}}_e), \quad (38a)$$

$$(\boldsymbol{\varepsilon}_e^0 + \dot{\boldsymbol{\varepsilon}}_e) + (\boldsymbol{\varepsilon}_p^0 + \dot{\boldsymbol{\varepsilon}}_p) = B(\mathbf{u}^0 + \dot{\mathbf{u}}), \quad (38b)$$

$$B^* \cdot (\boldsymbol{\sigma}^0 + \dot{\boldsymbol{\sigma}}) = \mathbf{t}^0 + \dot{\mathbf{t}}, \quad (38c)$$

$$\mathbf{u}_j^0 + \dot{\mathbf{u}}_j = \bar{\mathbf{u}}_j \quad (j \in J_u), \quad \mathbf{t}_j^0 + \dot{\mathbf{t}}_j = \bar{\mathbf{t}}_j \quad (j \in J_t), \quad (38d)$$

$$\boldsymbol{\eta}_q = \text{dev}(\boldsymbol{\sigma}_q^0 + \dot{\boldsymbol{\sigma}}_q) - (\boldsymbol{\beta}_q^0 + \dot{\boldsymbol{\beta}}_q), \quad (38e)$$

$$\dot{\boldsymbol{\varepsilon}}_{pq} = \gamma_q \frac{\boldsymbol{\eta}_q}{\|\boldsymbol{\eta}_q\|}, \quad \dot{\boldsymbol{\beta}}_q = \sqrt{\frac{2}{3}} s_{Kq} \frac{\boldsymbol{\eta}_q}{\|\boldsymbol{\eta}_q\|}, \quad (38f)$$

$$s_{Iq} = \sqrt{\frac{2}{3}} \theta H \gamma_q, \quad (38g)$$

$$s_{Kq} = \sqrt{\frac{2}{3}} (1 - \theta) H \gamma_q, \quad (38h)$$

$$\gamma_q \geq 0, \quad \|\boldsymbol{\eta}_q\| - \sqrt{\frac{2}{3}} (R_q^0 + s_{Iq}) \leq 0, \quad \gamma_q \left[\|\boldsymbol{\eta}_q\| - \sqrt{\frac{2}{3}} (R_q^0 + s_{Iq}) \right] = 0. \quad (38i)$$

Note again that the unknown variables in (38) are $\dot{\boldsymbol{\varepsilon}}_e$, $\dot{\boldsymbol{\varepsilon}}_p$, $\dot{\boldsymbol{\sigma}}$, $\dot{\mathbf{u}}$, $\dot{\mathbf{t}}$, $\dot{\boldsymbol{\beta}}$, $\boldsymbol{\eta}$, γ , s_I , and s_K . The conditions (38e)–(38i) should be satisfied for any $q = 1, \dots, n^G$, but we often omit to show it explicitly in the equations in order to simplify the presentation, if it is clear from the context.

4.2 Minimization problem of potential energy

Since we assume the associated flow rule, the minimization principles of the potential energy and the complementary energy can be formulated for the incremental problem [11, 32]. The principle of potential energy involves only the kinematic variables as unknowns. In section 3 we have seen that the plasticity law is formulated as the pair of SOCC conditions; see Proposition 3 and Proposition 4. We here focus on the inequality constraints of the kinematic variables involved in those SOCC conditions, i.e. (29) and (33). Besides the compatibility condition, say (38b), we introduce (29) and (33) as the constraint conditions of the minimization problem of the potential energy. This is a fundamental idea to formulate an SOCP problem which is equivalent to the incremental problem (38).

As the objective function, we consider the sum of the increments of the elastic potential energy and the plastic dissipation; see, e.g. [32]. In our case, the increment of the potential energy, in the presence of the isotropic and kinematic hardening, is defined by

$$\begin{aligned} \dot{II}(\dot{\boldsymbol{\varepsilon}}_e, \dot{\boldsymbol{\varepsilon}}_p, \dot{\mathbf{u}}, \gamma, \hat{\gamma}) \\ = \sum_{q=1}^{n^G} \left(\frac{1}{2} \dot{\boldsymbol{\varepsilon}}_{eq} : C_q : \dot{\boldsymbol{\varepsilon}}_{eq} + \boldsymbol{\varepsilon}_{eq}^0 : C_q : \dot{\boldsymbol{\varepsilon}}_{eq} + \boldsymbol{\beta}_q^0 : \dot{\boldsymbol{\varepsilon}}_{pq} \right. \\ \left. + \sqrt{\frac{2}{3}} R_q^0 \gamma_q + \frac{1}{3} \theta H \gamma_q^2 + \frac{1}{3} (1 - \theta) H \hat{\gamma}_q^2 \right) - \sum_{j \in J_t} \bar{\mathbf{t}}_j \dot{\mathbf{u}}_j. \end{aligned} \quad (39)$$

Note that \dot{II} is a convex quadratic function. Furthermore, γ and $\hat{\gamma}$ represent the plastic strain rates concerning the isotropic and kinematic hardening, respectively; see section 4.3 for detail.

The minimization problem of the potential energy is then formulated as

$$(PE) : \quad \min_{\dot{\boldsymbol{\varepsilon}}_e, \dot{\boldsymbol{\varepsilon}}_p, \dot{\boldsymbol{u}}, \gamma, \hat{\gamma}} \quad \dot{\Pi}(\dot{\boldsymbol{\varepsilon}}_e, \dot{\boldsymbol{\varepsilon}}_p, \dot{\boldsymbol{u}}, \gamma, \hat{\gamma}) \quad (40a)$$

$$\text{s. t.} \quad (\boldsymbol{\varepsilon}_e^0 + \dot{\boldsymbol{\varepsilon}}_e) + (\boldsymbol{\varepsilon}_p^0 + \text{dev}(\dot{\boldsymbol{\varepsilon}}_p)) = B(\boldsymbol{u}^0 + \dot{\boldsymbol{u}}), \quad (40b)$$

$$u_j^0 + \dot{u}_j = \bar{u}_j, \quad \forall j \in J_u, \quad (40c)$$

$$\gamma_q \geq \| -\dot{\boldsymbol{\varepsilon}}_{pq} \|, \quad \forall q, \quad (40d)$$

$$\hat{\gamma}_q \geq \| -\dot{\boldsymbol{\varepsilon}}_{pq} \|, \quad \forall q. \quad (40e)$$

Note that the constraint conditions (40d) and (40e) are in the same form. As we see below soon, the optimal values of γ_q and $\hat{\gamma}_q$ coincide, but they should be treated as independent variables in the problem (40).

It is emphasized that the problem (40) consists of the convex quadratic objective function, the linear equality constraints (in (40b) and (40c)), and the second-order cone constraints (in (40d) and (40e)). Thus the problem (40) is a convex optimization problem. Furthermore, as shown in section 4.5 below, the problem (40) can be reduced to an SOCP problem.

4.3 Optimality conditions

As seen in the preceding section, the problem (40) is a convex optimization problem. Moreover, it is easy to see that there always exists a strictly feasible solution, because γ_q and $\hat{\gamma}_q$ are not bounded from above. If we assume the existence of a solution to the force-balance equation, say (38c) and (38d), then the problem dual to (40) is also shown to be strictly feasible; see (46) below for the dual problem. Consequently, the Karush–Khun–Tacker (KKT) condition for (40) corresponds to the necessary and sufficient condition for the optimality.

We define the Lagrangian for the problem (40) as the function L takes the value

$$\begin{aligned} L = & \Pi(\dot{\boldsymbol{\varepsilon}}_e, \dot{\boldsymbol{\varepsilon}}_p, \dot{\boldsymbol{u}}, \gamma, \hat{\gamma}) - \dot{\boldsymbol{\sigma}} : [(\boldsymbol{\varepsilon}_e^0 + \dot{\boldsymbol{\varepsilon}}_e) + (\boldsymbol{\varepsilon}_p^0 + \text{dev}(\dot{\boldsymbol{\varepsilon}}_p)) - B(\boldsymbol{u}^0 + \dot{\boldsymbol{u}})] \\ & - \sum_{j \in J_t} \dot{t}_j (u_j^0 + \dot{u}_j - \bar{u}_j) - \sum_{q=1}^{n^G} (\lambda_q \gamma_q - \boldsymbol{\eta}_q : \dot{\boldsymbol{\varepsilon}}_{pq}) - \sum_{q=1}^{n^G} (\mu_q \hat{\gamma}_q - \dot{\boldsymbol{\beta}}_q : \dot{\boldsymbol{\varepsilon}}_{pq}) \end{aligned} \quad (41)$$

if $\lambda_q \geq \|\boldsymbol{\eta}_q\|$, $\mu_q \geq \|\dot{\boldsymbol{\beta}}_q\|$ ($\forall q$), otherwise we put $L = -\infty$. Here, $\dot{\boldsymbol{\sigma}}$, \dot{t}_j ($j \in J_t$), $\dot{\boldsymbol{\beta}}_q$, $\boldsymbol{\eta}$, λ , and μ are the Lagrange multipliers. As the stationary condition of L , the KKT condition for the

problem (40) is obtained as

$$\boldsymbol{\sigma}^0 + \dot{\boldsymbol{\sigma}} = C : (\boldsymbol{\varepsilon}_e^0 + \dot{\boldsymbol{\varepsilon}}_e), \quad (42a)$$

$$(\boldsymbol{\varepsilon}_e^0 + \dot{\boldsymbol{\varepsilon}}_e) + (\boldsymbol{\varepsilon}_p^0 + \text{dev}(\dot{\boldsymbol{\varepsilon}}_p)) = B(\mathbf{u}^0 + \dot{\mathbf{u}}), \quad (42b)$$

$$B^* \cdot (\boldsymbol{\sigma}^0 + \dot{\boldsymbol{\sigma}}) = \dot{\mathbf{t}}, \quad (42c)$$

$$u_j^0 + \dot{u}_j = \bar{u}_j \quad (j \in J_u), \quad t_j^0 + \dot{t}_j = \bar{t}_j \quad (j \in J_t), \quad (42d)$$

$$\boldsymbol{\beta}_q^0 - \text{dev}(\boldsymbol{\sigma})_q + \boldsymbol{\eta}_q + \dot{\boldsymbol{\beta}}_q = \mathbf{o}, \quad (42e)$$

$$\lambda_q = \sqrt{\frac{2}{3}} R_q^0 + \frac{2}{3} \theta H \gamma_q, \quad (42f)$$

$$\mu_q = \frac{2}{3} (1 - \theta) H \hat{\gamma}_q, \quad (42g)$$

$$\lambda_q \geq \|\boldsymbol{\eta}_q\|, \quad \gamma_q \geq \|\dot{\boldsymbol{\varepsilon}}_{pq}\|, \quad \lambda_q \gamma_q - \boldsymbol{\eta}_q : \dot{\boldsymbol{\varepsilon}}_{pq} = 0, \quad (42h)$$

$$\mu_q \geq \|\dot{\boldsymbol{\beta}}_q\|, \quad \hat{\gamma}_q \geq \|\dot{\boldsymbol{\varepsilon}}_{pq}\|, \quad \mu_q \hat{\gamma}_q - \dot{\boldsymbol{\beta}}_q : \dot{\boldsymbol{\varepsilon}}_{pq} = 0, \quad (42i)$$

where $\boldsymbol{\sigma}^0$ and \mathbf{t}^0 are defined by

$$\begin{aligned} \boldsymbol{\sigma}^0 &= C : \boldsymbol{\varepsilon}_e^0, \\ \mathbf{t}^0 &= B^* \cdot \boldsymbol{\sigma}^0. \end{aligned}$$

In what follows, we show that (42) is equivalent to (38) to guarantee that solving the problem (40) is truly equivalent to solving the incremental problem (38). To this end, it suffices to show that (42b), (42f)–(42i) are equivalent to (38b), (38f)–(38i).

By substituting (15) and (16) into (42f) and (42g), respectively, we obtain

$$\lambda_q = \sqrt{\frac{2}{3}} (R_q^0 + s_{Iq}), \quad (43)$$

$$\mu_q = \sqrt{\frac{2}{3}} s_{Kq}. \quad (44)$$

From the definition (39), we see that the objective function \dot{I} of the problem (40) increases monotonically with respect to γ_q and $\hat{\gamma}_q$. Therefore, at the optimal solution, the constraints (40d) and (40e) are satisfied as the equalities

$$\gamma_q = \hat{\gamma}_q = \|\dot{\boldsymbol{\varepsilon}}_{pq}\|,$$

i.e. γ_q and $\hat{\gamma}_q$ share the same value at the optimal solution. From this observation, and using (43) and (44), we can rewrite (42h) and (42i) equivalently as

$$\sqrt{\frac{2}{3}} (R_q^0 + s_{Iq}) \geq \|\boldsymbol{\eta}_q\|, \quad \gamma_q \geq \|\dot{\boldsymbol{\varepsilon}}_{pq}\|, \quad \sqrt{\frac{2}{3}} (R_q^0 + s_{Iq}) \gamma_q - \boldsymbol{\eta}_q : \dot{\boldsymbol{\varepsilon}}_{pq} = 0, \quad (45a)$$

$$\sqrt{\frac{2}{3}} s_{Kq} \geq \|\dot{\boldsymbol{\beta}}_q\|, \quad \gamma_q \geq \|\dot{\boldsymbol{\varepsilon}}_{pq}\|, \quad \sqrt{\frac{2}{3}} s_{Kq} \gamma_q - \dot{\boldsymbol{\beta}}_q : \dot{\boldsymbol{\varepsilon}}_{pq} = 0. \quad (45b)$$

Note that (45a) and (45b) are the SOCC conditions. It follows from Proposition 3 that (45a) is equivalent to the flow rule in conjunction with the isotropic hardening, i.e. (5), (15), and (19). Moreover, from Proposition 4 we see that (45b) is equivalent to the kinematic hardening rule, i.e. (16) and (18). Consequently, (45a) and (45b), and hence (42h) and (42i) also, are equivalent to (38f)–(38i).

We thus have shown that (42h) and (42i) imply the plasticity law, say (1), (5), and (15)–(19). The remainder is to show that the plasticity law implies $\text{dev}(\dot{\boldsymbol{\varepsilon}}_p) = \dot{\boldsymbol{\varepsilon}}_p$ in order to see that (42b) can be replaced with (38b) without loss of generality. As seen in section 2, the plasticity law implies (11). Therefore, from (5) we obtain $\text{tr}(\dot{\boldsymbol{\varepsilon}}_{pq}) = 0$, and hence $\text{dev}(\dot{\boldsymbol{\varepsilon}}_p) = \dot{\boldsymbol{\varepsilon}}_p$. Consequently, (42h) and (42i) imply $\text{dev}(\dot{\boldsymbol{\varepsilon}}_p) = \dot{\boldsymbol{\varepsilon}}_p$, and hence we can replace $\text{dev}(\dot{\boldsymbol{\varepsilon}}_p)$ in (42b) with $\dot{\boldsymbol{\varepsilon}}_p$ without loss of generality.

In this way, (42) is equivalent to (38). Therefore, the solution of the incremental problem (38) can be truly obtained by solving the problem (40).

4.4 Minimization problem of complementary energy

The problem dual to (40) is formulated as the optimization problem whose KKT condition coincides with (42). For explicitly describing the dual problem with the physical meaning, we use (43) and (44) to replace the Lagrange multipliers λ_q and μ_q with variables s_{Iq} and s_{Kq} , respectively. Then the problem dual to (40) can be formulated in the variables $\dot{\boldsymbol{\sigma}}, \dot{\boldsymbol{t}}, \dot{\boldsymbol{\beta}}, \boldsymbol{\eta}, s_I$, and s_K as

$$\text{(CE)} \quad \min_{\dot{\boldsymbol{\sigma}}, \dot{\boldsymbol{t}}, \dot{\boldsymbol{\beta}}, \boldsymbol{\eta}, s_I, s_K} \quad \dot{I}_c(\dot{\boldsymbol{\sigma}}, \dot{\boldsymbol{t}}, \dot{\boldsymbol{\beta}}, \boldsymbol{\eta}, s_I, s_K) \quad (46a)$$

$$\text{s. t.} \quad B^* \cdot (\boldsymbol{\sigma}^0 + \dot{\boldsymbol{\sigma}}) = \boldsymbol{t}^0 + \dot{\boldsymbol{t}}, \quad (46b)$$

$$t_j^0 + \dot{t}_j = \bar{t}_j, \quad \forall j \in J_t, \quad (46c)$$

$$\boldsymbol{\eta}_q = \text{dev}(\boldsymbol{\sigma}_q^0 + \dot{\boldsymbol{\sigma}}_q) - (\boldsymbol{\beta}_q^0 + \dot{\boldsymbol{\beta}}_q), \quad \forall q, \quad (46d)$$

$$\sqrt{\frac{2}{3}}(R_q^0 + s_{Iq}) \geq \|\boldsymbol{\eta}_q\|, \quad \forall q, \quad (46e)$$

$$\sqrt{\frac{2}{3}}s_{Kq} \geq \|\dot{\boldsymbol{\beta}}_q\|, \quad \forall q, \quad (46f)$$

where \dot{I}_c is defined by

$$\begin{aligned} & \dot{I}_c(\dot{\boldsymbol{\sigma}}, \dot{\boldsymbol{t}}, \dot{\boldsymbol{\beta}}, \boldsymbol{\eta}, s_I, s_K) \\ &= \sum_{q=1}^{n_G} \left(\frac{1}{2} \dot{\boldsymbol{\sigma}}_q : C_q^{-1} : \dot{\boldsymbol{\sigma}}_q + \boldsymbol{\sigma}_q^0 : C_q^{-1} : \dot{\boldsymbol{\sigma}}_q + \boldsymbol{\varepsilon}_{pq}^0 : \dot{\boldsymbol{\sigma}}_q \right. \\ & \quad \left. + \frac{1}{2\theta H} s_{Iq}^2 + \frac{1}{2(1-\theta)H} s_{Kq}^2 \right) - \sum_{j \in J_u} \bar{u}_j \dot{t}_j. \end{aligned} \quad (47)$$

Note that we formulate the problem (46) as a minimization problem following the conventional way to state the complementary energy principle as a minimum principle.

It is emphasized that the problem (46) consists of the convex quadratic objective function, the linear equality constraints (in (46b), (46c), and (46d)), and the second-order cone constraints (in (46e) and (46f)). Therefore, like the problem (40), the problem (46) is a convex optimization problem, which can be solved effectively. In this paper we propose to solve the pair of (40) and (46) by using the primal-dual interior-point method for the SOCP.

It is noted that the problem (46) involves only the static variables, in contrast to the problem (40) which involves only kinematic variables. Thus the problem (46) serves as the minimization problem of the complementary energy, and \dot{I}_c defined by (47) is regarded as the complementary energy function. Moreover, if (46b) and (46c) have a solution, then the problem (46)

has a strictly feasible solution, because s_{I_q} and s_{K_q} are not bounded from above. Since \dot{I}_c increases monotonically with respect to s_{I_q} and s_{K_q} , the constraints (46e) and (46f) are satisfied as equalities at the optimal solution. It is also emphasized that the conditions

$$\text{tr}(\dot{\boldsymbol{\varepsilon}}_{pq}) = 0, \quad \text{tr}(\dot{\boldsymbol{\beta}}_q) = 0, \quad \text{tr}(\boldsymbol{\eta}_q) = 0$$

are not involved explicitly in the problems (40) nor (46) as constraints. Nonetheless, they are guaranteed to be satisfied at their optimal solutions, because the optimal solutions satisfy the SOCC conditions in Proposition 2 and Proposition 3.

4.5 Reduction to second-order cone programming problem

Through the discussion above it has been shown that the solution of the incremental problem can be obtained by solving the primal-dual pair of SOCP problems, say (40) and (46). Each of these problem is a minimization problem of a convex quadratic function over some linear equality constraints and second-order cone constraints. It is known that such an optimization problem can further be reduced to an SOCP problem, which is a minimization problem of a linear function over some linear equality constraints and second-order cone constraints. Therefore, we propose to solve (40) and (46) by applying the primal-dual interior-point method for SOCP [1, 4].

Since the treatment of the convex quadratic objective function within the framework of second-order cone can be found in textbooks, e.g. [4], we here show only the fundamental idea. As an example, consider the primal problem (40). In the objective function defined by (39), the terms

$$\frac{1}{2}\dot{\boldsymbol{\varepsilon}}_{eq} : C : \dot{\boldsymbol{\varepsilon}}_{eq}, \quad \frac{1}{3}\theta H \gamma_q^2, \quad \frac{1}{3}(1 - \theta)H \hat{\gamma}_q^2$$

are quadratic. Since problem (40) is a minimization problem, we consider, for example, the minimization of the first term. By using the Voigt notation, the strain tensor $\boldsymbol{\varepsilon} \in \mathcal{S}$ is put in a vector form as

$$\mathbf{vec}(\boldsymbol{\varepsilon}) = (\varepsilon_{11}, \varepsilon_{22}, \varepsilon_{33}, 2\varepsilon_{12}, 2\varepsilon_{23}, 2\varepsilon_{13})^T.$$

Furthermore, we introduce an auxiliary variable $t_q \in \mathbb{R}$ to rewrite the minimization of $\frac{1}{2}\dot{\boldsymbol{\varepsilon}}_{eq} : C_q : \dot{\boldsymbol{\varepsilon}}_{eq}$ as

$$\min_{\dot{\boldsymbol{\varepsilon}}_{eq}, t_q} t_q \tag{48a}$$

$$\text{s. t.} \quad t_q \geq \frac{1}{2} \mathbf{vec}(\dot{\boldsymbol{\varepsilon}}_{eq})^T \tilde{C}_q \mathbf{vec}(\dot{\boldsymbol{\varepsilon}}_{eq}), \tag{48b}$$

where $\tilde{C}_q \in \mathbb{R}^{6 \times 6}$ is the elasticity tensor in a matrix form. Because of the positive definiteness of the elasticity tensor, \tilde{C}_q is a symmetric positive definite matrix. Therefore, there exists a matrix $G_q \in \mathbb{R}^{6 \times 6}$ satisfying $G_q^T G_q = \tilde{C}_q$. By using G_q , the problem (48) can be reformulated as

$$\begin{aligned} & \min_{\dot{\boldsymbol{\varepsilon}}_{eq}, t_q} t_q \\ & \text{s. t.} \quad t_q + (1/2) \geq \left\| \begin{bmatrix} t_q - (1/2) \\ G_q \mathbf{vec}(\dot{\boldsymbol{\varepsilon}}_{eq}) \end{bmatrix} \right\|, \end{aligned}$$

which is an SOCP problem. In this way, we can restate the nonlinear terms involved in the objective functions of (40) and (46) with some second-order cone constraints to obtain SOCP formulations.

5 Warm-start strategy

We have shown in section 4 that the solution of incremental problem for the quasistatic elastoplastic analysis can be found by solving the primal-dual pair of SOCP problems, i.e. (40) and (46). This pair of problems are solved efficiently by using the polynomial-time primal-dual interior-point method with guaranteed convergence to the solution.

Because of the irreversible property of the plasticity, the elastoplastic analysis should be performed stepwise by dividing the time interval $[0, T]$ into sufficiently small subintervals. Once the solution of the incremental problem for a specific subinterval, say $[\tau_0, \tau_1]$, is obtained, then we turn towards new incremental problem for the next time subinterval $[\tau_1, \tau_2]$ by updating the boundary conditions, i.e. \bar{u}_j ($j \in J_u$) and \bar{t}_j ($j \in J_t$), as well as the state variables, i.e. β^0 , R^0 , ε_e^0 , ε_p^0 , σ^0 , \mathbf{u}^0 , and \mathbf{t}^0 . It is usual that the change in these problem data is small. Thus in the elastoplastic analysis we solve a series of closely related problems, and hence we may expect that the difference between the solutions at τ_1 and τ_2 is also small. The warm-start strategy proposed in this section is to make use of the solution at the loading step τ_1 to solve the problem for the loading step τ_2 in order to reduce the computational effort required by the primal-dual interior-point method for SOCP in the course of the elastoplastic analysis.

5.1 Problem setting

To begin, we define a *parent problems*, which is the primal-dual pair of the SOCP problems solved at the previous loading step, say at time τ_1 . Let $\mathcal{K} \subset \mathbb{R}^n$ denote the cone defined by the direct product of the nonnegative orthant and some second-order cones. We write $\mathbf{x} \succeq_{\mathcal{K}} \mathbf{0}$ if $\mathbf{x} \in \mathcal{K}$. The parent problem, consisting of (Parent P) and (Parent D), is written in the abstract form as

$$\begin{array}{ll}
 \text{(Parent P)} & \text{(Parent D)} \\
 \min_{\mathbf{x}} & \mathbf{c}^T \mathbf{x} & \max_{\mathbf{y}, \mathbf{z}} & \mathbf{b}^T \mathbf{y} \\
 \text{s. t.} & A\mathbf{x} = \mathbf{b}, & \text{s. t.} & A^T \mathbf{y} + \mathbf{z} = \mathbf{c}, \\
 & \mathbf{x} \succeq_{\mathcal{K}} \mathbf{0}; & & \mathbf{z} \succeq_{\mathcal{K}} \mathbf{0},
 \end{array}$$

where $A \in \mathbb{R}^{m \times n}$, $\mathbf{x}, \mathbf{z} \in \mathbb{R}^n$ and $\mathbf{y}, \mathbf{b} \in \mathbb{R}^m$. We suppose that both (Parent P) and (Parent D) have strictly feasible solutions.

Let \mathbf{x}^* and $(\mathbf{y}^*, \mathbf{z}^*)$ denote the optimal solutions of (Parent P) and (Parent D), respectively. Then \mathbf{x}^* , \mathbf{y}^* , and \mathbf{z}^* satisfy the KKT condition

$$\begin{aligned}
 A\mathbf{x}^* &= \mathbf{b}, \\
 A^T \mathbf{y}^* + \mathbf{z}^* &= \mathbf{c}, \\
 \mathbf{x}^* \succeq_{\mathcal{K}} \mathbf{0}, \quad \mathbf{z}^* \succeq_{\mathcal{K}} \mathbf{0}, \quad \mathbf{x}^{*\top} \mathbf{z}^* &= 0.
 \end{aligned}$$

From the practical point of view, we may assume that \mathbf{x}^* and \mathbf{z}^* are on the boundary of \mathcal{K} , i.e.

$$\mathbf{x}^* \notin \text{int } \mathcal{K}, \quad \mathbf{z}^* \notin \text{int } \mathcal{K}.$$

Although an approximate optimal solution obtained by the primal-dual interior-point methods is usually an interior point of \mathcal{K} in a precise sense, the point is very close to the boundary so that

widely-used solvers, such as SDPT3 [39] or SDPA [41], recognize it as boundary points when it is provided as an initial solution. Hence, in what follows we regard \mathbf{x}^* and \mathbf{z}^* as boundary points.

After solving the parent problem, we proceed to solve a new incremental problem for the next loading step, i.e. for the loading step τ_2 . The pair of SOCP problems to be solved is called the *child problem*, which is written in the abstract form as

$$\begin{array}{ll}
\text{(Child P)} & \text{(Child D)} \\
\min_{\mathbf{x}} & \tilde{\mathbf{c}}^T \mathbf{x} & \max_{\mathbf{y}, \mathbf{z}} & \tilde{\mathbf{b}}^T \mathbf{y} \\
\text{s. t.} & \tilde{A} \mathbf{x} = \tilde{\mathbf{b}}, & \text{s. t.} & \tilde{A}^T \mathbf{y} + \mathbf{z} = \tilde{\mathbf{c}}, \\
& \mathbf{x} \succeq_{\mathcal{K}} \mathbf{0}; & & \mathbf{z} \succeq_{\mathcal{K}} \mathbf{0}.
\end{array}$$

Here, \tilde{A} , $\tilde{\mathbf{b}}$ and $\tilde{\mathbf{c}}$ are slightly perturbed from A , \mathbf{b} and \mathbf{c} , but are of the same sizes. The cone \mathcal{K} is also common between the parent and child problems. Suppose that both (Child P) and (Child D) are strictly feasible. Let \mathbf{x}^{opt} and $(\mathbf{y}^{\text{opt}}, \mathbf{z}^{\text{opt}})$ denote the optimal solutions of (Child P) and (Child D), respectively. We aim to make use of \mathbf{x}^* and $(\mathbf{y}^*, \mathbf{z}^*)$ for warm-starting the primal-dual interior-point method solving the pair of (Child P) and (Child D) in order to reduce the computational effort required at the current loading step τ_2 .

In the context of the elastoplastic analysis, unfortunately, \mathbf{x}^* and $(\mathbf{y}^*, \mathbf{z}^*)$ are not feasible for (Child P) and (Child D) in general. Moreover, \mathbf{x}^* and \mathbf{z}^* are not interior points of \mathcal{K} . From these reasons, a crude warm-start strategy, in which we directly use $(\mathbf{x}^*, \mathbf{y}^*, \mathbf{z}^*)$ as an initial point for the interior-point method to solve (Child P) and (Child D), is entirely inefficient; see, e.g. the discussion in [2] for the case of LP. On the other hand, we prefer to employ the available well-developed software packages of the primal-dual interior-point methods [39, 41], rather than to implement a new algorithm specifically designed for warm start. Therefore, we have chosen the following strategy for warm start: (i) We firstly formulate a penalized problem, which are a primal-dual pair of SOCP problems, sharing the same optimal solution as the child problem; (ii) secondly, by using $(\mathbf{x}^*, \mathbf{y}^*, \mathbf{z}^*)$, we construct an initial point which is strictly feasible for the penalized problem; (iii) we start an interior-point solver from the initial point to solve the penalized problem, and then obtain the optimal solution of the child problem. In the succeed section we propose the penalized problem as well as its good initial point.

5.2 Penalized problems and warm-start strategy

For fully enjoying the advantage of the primal-dual interior-point methods, we introduce relaxations both for (Child P) and (Child D) to construct a penalized problem. The following

penalized problem which we propose consists of a pair of primal and dual SOCP problems:

$$\begin{array}{ll}
\text{(Penalty P)} & \text{(Penalty D)} \\
\min_{\mathbf{x}, \xi, v, \mathbf{w}} & \tilde{\mathbf{c}}^T \mathbf{x} + M_1 \xi + M_2 v & \max_{\mathbf{y}, \mathbf{z}, \zeta} & \tilde{\mathbf{b}}^T \mathbf{y} - M_3 \zeta \\
\text{s. t.} & \tilde{A} \mathbf{x} + \mathbf{w} = \tilde{\mathbf{b}}, & \text{s. t.} & \tilde{A}^T \mathbf{y} + \mathbf{z} = \tilde{\mathbf{c}}, \\
& \mathbf{x} + \xi \mathbf{1} \succeq_{\mathcal{K}} \mathbf{0}, & & \mathbf{z} + \zeta \mathbf{1} \succeq_{\mathcal{K}} \mathbf{0}, \\
& \xi \geq 0, & & \zeta \geq 0, \\
& M_3 - (\mathbf{x} + \xi \mathbf{1})^T \mathbf{1} \geq 0, & & M_1 - \mathbf{z}^T \mathbf{1} \geq 0, \\
& v \geq \|\mathbf{w}\|; & & M_2 \geq \|\mathbf{y}\|,
\end{array}$$

where M_1, M_2 and $M_3 > 0$ are sufficiently large constants which serve as the penalty parameters, while $\xi, v, \zeta \in \mathbb{R}$ and $\mathbf{w} \in \mathbb{R}^m$ are auxiliary variables. The vector $\mathbf{1} \in \mathcal{K}$ is the identity element of the Jordan algebra associated with \mathcal{K} ; for example, if \mathcal{K} is given by

$$\mathcal{K} = \mathbb{R}_+^2 \times \{(p_1, \mathbf{q}_1) \in \mathbb{R}^3 \mid p_1 \geq \|\mathbf{q}_1\|\} \times \{(p_2, \mathbf{q}_2) \in \mathbb{R}^4 \mid p_2 \geq \|\mathbf{q}_2\|\},$$

then $\mathbf{1}$ is the 9-dimensional vector defined by

$$\mathbf{1} = (1, 1, 1, 0, 0, 1, 0, 0, 0)^T.$$

Note that \mathbf{w} serves as the relaxation variables vector for the equality constraints of (Child P), while ξ and ζ are the relaxation variables for the conic inequality constraints, say “ $\succeq_{\mathcal{K}}$ ”, in (Child P) and (Child D), respectively.

The optimal solution of (Child P) and (Child D) can be obtained from the optimal solutions of (Penalty P) and (Penalty D) in the following manner.

Proposition 5. *Suppose that M_1, M_2 , and M_3 are sufficiently large, and that (Child P) and (Child D) are strictly feasible. Then \mathbf{x}^{opt} and $(\mathbf{y}^{\text{opt}}, \mathbf{z}^{\text{opt}})$ are optimal for (Child P) and (Child D), respectively, if and only if $(\mathbf{x}, \xi, v, \mathbf{w})$ and $(\mathbf{y}, \mathbf{z}, \zeta)$ defined by*

$$\mathbf{x} = \mathbf{x}^{\text{opt}}, \quad \xi = 0, \quad v = 0, \quad \mathbf{w} = \mathbf{0}, \quad (49a)$$

$$\mathbf{y} = \mathbf{y}^{\text{opt}}, \quad \mathbf{z} = \mathbf{z}^{\text{opt}}, \quad \zeta = 0 \quad (49b)$$

are optimal for (Penalty P) and (Penalty D), respectively.

Proof. It is easily seen that the strict feasibility of (Child P) and (Child D) implies those of (Penalty P) and (Penalty D). Since all these problems are SOCPs, their optimality conditions are given by the KKT conditions.

Concerning (Child P) and (Child D), the optimal solutions, say \mathbf{x}^{opt} and $(\mathbf{y}^{\text{opt}}, \mathbf{z}^{\text{opt}})$, satisfy the following KKT condition:

$$\tilde{A} \mathbf{x}^{\text{opt}} = \tilde{\mathbf{b}}, \quad (50a)$$

$$\tilde{A}^T \mathbf{y}^{\text{opt}} + \mathbf{z}^{\text{opt}} = \tilde{\mathbf{c}}, \quad (50b)$$

$$\mathbf{x}^{\text{opt}} \succeq_{\mathcal{K}} \mathbf{0}, \quad \mathbf{z}^{\text{opt}} \succeq_{\mathcal{K}} \mathbf{0}, \quad \mathbf{x}^{\text{opt}T} \mathbf{z}^{\text{opt}} = 0. \quad (50c)$$

Similarly, $(\mathbf{x}, \xi, v, \mathbf{w})$ and $(\mathbf{y}, \mathbf{z}, \zeta)$ are optimal for (Penalty P) and (Penalty D) if and only if they satisfy

$$\tilde{A}\mathbf{x} + \mathbf{w} = \tilde{\mathbf{b}}, \quad (51a)$$

$$\tilde{A}^T\mathbf{y} + \mathbf{z} = \tilde{\mathbf{c}}, \quad (51b)$$

$$\mathbf{x} + \xi\mathbf{1} \succeq_{\mathcal{K}} \mathbf{0}, \quad \mathbf{z} + \zeta\mathbf{1} \succeq_{\mathcal{K}} \mathbf{0}, \quad (\mathbf{x} + \xi\mathbf{1})^T(\mathbf{z} + \zeta\mathbf{1}) = 0, \quad (51c)$$

$$\xi \geq 0, \quad M_1 - \mathbf{z}^T\mathbf{1} \geq 0, \quad \xi(M_1 - \mathbf{z}^T\mathbf{1}) = 0, \quad (51d)$$

$$M_3 - \mathbf{1}^T\mathbf{x} - (\mathbf{1}^T\mathbf{1})\xi \geq 0, \quad \zeta \geq 0, \quad [M_3 - \mathbf{1}^T\mathbf{x} - (\mathbf{1}^T\mathbf{1})\xi]\zeta = 0, \quad (51e)$$

$$v \geq \|\mathbf{w}\|, \quad M_2 \geq \|\mathbf{y}\|, \quad M_2v + \mathbf{w}^T\mathbf{y} = 0. \quad (51f)$$

Since M_1 , M_2 , and M_3 are sufficiently large, we may assume that \mathbf{x}^{opt} , \mathbf{y}^{opt} , and \mathbf{z}^{opt} satisfy

$$M_1 - \mathbf{1}^T\mathbf{z}^{\text{opt}} > 0, \quad (52a)$$

$$M_3 - \mathbf{1}^T\mathbf{x}^{\text{opt}} > 0, \quad (52b)$$

$$M_2 > \|\mathbf{y}^{\text{opt}}\|. \quad (52c)$$

Therefore, if we put $\mathbf{x} = \mathbf{x}^{\text{opt}}$, $\mathbf{y} = \mathbf{y}^{\text{opt}}$, and $\mathbf{z} = \mathbf{z}^{\text{opt}}$ in (51), then (51d)–(51f) and (52) imply $\xi = v = \zeta = 0$ and $\mathbf{w} = \mathbf{0}$. Thus all the relaxation variables vanish, and hence the solution defined by (49) satisfies (51). \square

Proposition 5 justifies solving (Penalty P) and (Penalty D) instead of (Child P) and (Child D). Indeed, if the obtained optimal solutions of (Penalty P) and (Penalty D) satisfies $\xi = v = \zeta = \|\mathbf{w}\| = 0$, then we can see that M_1 , M_2 , and M_3 have been chosen appropriately in the sense that the optimal solutions of (Child P) and (Child D) are successfully obtained.

For solving the penalized problem by using the primal-dual interior-point method, it is preferred to give an interior feasible point which is expected to be close to the optimal point. The condition (49) in Proposition 5 suggests a good initial point for the penalized problem; because $(\mathbf{x}^{\text{opt}}, \mathbf{y}^{\text{opt}}, \mathbf{z}^{\text{opt}})$ is expected to be close to $(\mathbf{x}^*, \mathbf{y}^*, \mathbf{z}^*)$, the optimal solutions of (Penalty P) and (Penalty D) may be close to $(\mathbf{x}^*, 0, 0, \mathbf{0})$ and $(\mathbf{y}^*, \mathbf{z}^*, 0)$, respectively. Accordingly, we construct initial solutions $(\mathbf{x}^0, \xi^0, v^0, \mathbf{w}^0)$ and $(\mathbf{y}^0, \mathbf{z}^0, \zeta^0)$ as

$$\mathbf{x}^0 = \mathbf{x}^*, \quad \xi^0 = \varepsilon_x, \quad v^0 = \|\mathbf{w}^0\| + \varepsilon_x, \quad \mathbf{w}^0 = \tilde{\mathbf{b}} - \tilde{A}\mathbf{x}^0, \quad (53a)$$

$$\mathbf{y}^0 = \mathbf{y}^*, \quad \mathbf{z}^0 = \tilde{\mathbf{c}} - \tilde{A}^T\mathbf{y}^*, \quad \zeta^0 = \min \{ \zeta \mid \mathbf{z}^0 + \zeta\mathbf{1} \succeq_{\mathcal{K}} \varepsilon_z\mathbf{1} \}, \quad (53b)$$

where $\varepsilon_x > 0$ and $\varepsilon_z > 0$ are small constants; see Remark 6. It is easy to see that $(\mathbf{x}^0, \xi^0, v^0, \mathbf{w}^0)$ and $(\mathbf{y}^0, \mathbf{z}^0, \zeta^0)$ defined by (53) are strictly feasible for (Penalty P) and (Penalty D), respectively.

Remark 6. In (53), ε_x and ε_z are positive constants guaranteeing that the initial point is in the interior of \mathcal{K} . However, too large values of ε_x and ε_z make an initial point far from the optimal point of the penalized problem. Thus the computational efficiency depends on the choice of $(\varepsilon_x, \varepsilon_z)$. In the numerical examples in section 6, we set

$$\varepsilon_x = 0.1 \frac{\|\mathbf{x}^0\|}{n}, \quad \varepsilon_z = 0.1 \frac{\|\mathbf{z}^0\|}{n}, \quad (54)$$

which are suggested to be reasonable by our preliminary experiments. \blacksquare

Remark 7. The penalty parameters M_1 , M_2 , and M_3 should be chosen so as to satisfy (52), although we do not know \mathbf{x}^{opt} , \mathbf{y}^{opt} , and \mathbf{z}^{opt} in advance. On the other hand, too large penalty parameters may possibly cause the numerical instability. Hence, we attempt to estimate appropriate values for the penalty parameters by using the optimal point of the parent problem, say $(\mathbf{x}^{\text{opt}}, \mathbf{y}^{\text{opt}}, \mathbf{z}^{\text{opt}})$. Based on (52), we set

$$\begin{aligned} M_1 &= 3.1(\mathbf{1}^T \mathbf{z}^*), \\ M_2 &= 3.1\|\mathbf{y}^*\|, \\ M_3 &= 1.1(\mathbf{1}^T \mathbf{x}^*), \end{aligned}$$

which are adopted in the numerical experiments presented in section 6. ■

In the elastoplastic analysis during the time interval $[0, T]$, we begin with solving the incremental problem for the first loading step by using the primal-dual interior-point method from cold start. At all the subsequent loading steps, we make use of the solution of the previous loading step for warm start, i.e. the penalized problem is solved at each loading step from the initial solution defined by (53) and (54). Such an initial point is a strictly feasible point of the penalized problem, and is expected to be close to the optimal solution of the penalized problem. Therefore, this warm-start strategy is expected to reduce the computational effort required by the primal-dual interior-point method.

6 Numerical experiments

Two elastoplastic problems are solved numerically by the proposed method. Computation has been carried out on Quad-Core Xeon E5450 (3.00 GHz with 16.0 GB memory) with MATLAB Ver. R2007b [35]. The SOCP problems are solved by using SDPT3 Ver. 4.20 [39], which implements the primal-dual infeasible interior-point method.

In the following examples, we consider the isotropic solids, where the elastic modulus and the Poisson ratio are 10.0 MPa and 0.2, respectively. The solids are discretized into 20-node serendipity isoparametric hexahedron elements with $2 \times 2 \times 2$ Gauss quadrature points [28]. The parameters for hardening rules in (12)–(14) are taken to be $\sigma^Y = 10.0$ kPa, $H = 200.0$ kPa, and $\theta = 0.5$.

6.1 Perforated plate

We consider a plate with a circular hole illustrated in Figure 1, which is in a state of plane strain. Numerical analysis is performed by using the three-dimensional hexahedron elements by fixing the nodal displacements in the thickness direction.

Due to the symmetry, only a quarter of the plate is modeled as shown in Figure 1 by 420 elements, which leads in total to 9549 degrees of freedom. The total number of Gauss evaluation points is $n^G = 3360$. The dimensions of this model are given as follows: The height is $\ell = 12.0$ cm, the width is 8.0 cm, the thickness is 1.0 cm, and the radius of the hole is 4.0 cm. As the loading condition, the displacements are prescribed as follows: The vertical displacement of the lower edge and the horizontal displacement of the left edge are fixed, the horizontal displacement of the

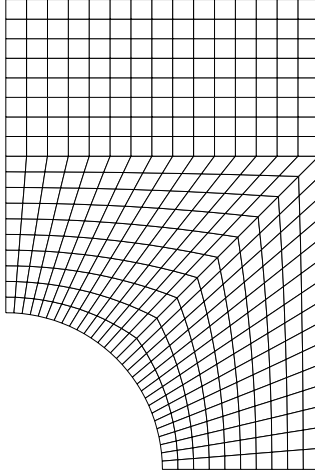


Figure 1: Plate with a circular hole (420 elements, 9549 degrees of freedom).

upper edge is free, and the vertical displacement of the upper edge, denoted $\bar{\mathbf{u}}_{\text{upper}}$, is prescribed. The history of $\bar{\mathbf{u}}_{\text{upper}}$ is given by $\bar{\mathbf{u}}_{\text{upper}} = r\ell/100$ with the parameter r .

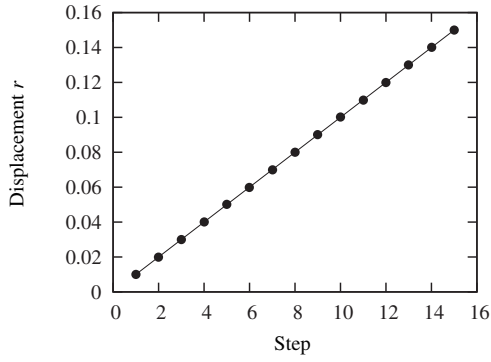
We firstly consider a monotonic loading, where the variation of r is defined by Figure 2(a). The obtained variation of reaction force is depicted in Figure 2(b). Figures 3(a) and (b) compare the the number of iterations and computational time at each loading step required by the conventional cold-start method and the proposed warm-start method. It can be seen that use of the warm-start strategy decreases the computational effort by more than half compared with cold start. To demonstrate the robustness of the proposed method, the same problem is resolved by using the five equal increments, where $\Delta r = 0.03$. The computational results are shown in Figures 3(c) and (d), where we can observed that the step size does not affect the efficiency of the proposed method. Figure 4 shows the evolution of the effective plastic strain, i.e. $\|\boldsymbol{\varepsilon}_p\|$, which agrees well with the numerical results in literature [32, 34].

Secondly, we examine a cyclic loading, where the variation of r is defined by Figure 5(a). The obtained load–displacement curve is depicted in Figure 5(b), where the Bauschinger effect is clearly observed. In Figure 6 we show the evolution of the effective plastic strain. Note that $\mathbf{u}_{\text{upper}}$ at the 2nd loading step depicted in Figure 6(a) is same as that at the 6th step in the monotonic loading case depicted in Figure 4(b), because in this cyclic loading test we use more coarse time-discretization.

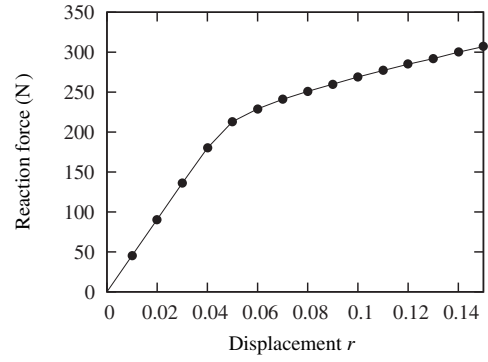
6.2 Tapered cylinder

We next consider a tapered cylinder illustrated in Figure 7. The cylinder is discretized into 480 hexahedron elements, which leads in total to the 6195 degrees of freedom and the 3840 Gauss points.

The dimensions of the cylinder is given as follows: The height of the cylinder is $\ell = 10.0$ cm, the radii of the lower and upper faces are 2.0 cm and 3.0 cm, respectively, where the lower 2/3-part of the cylinder is tapered. As the loading condition, we suppose that vertical displacement of the lower face is fixed, while the horizontal displacements of the upper and lower faces are free. The vertical displacement of the upper face is subjected to the prescribed increments defined by

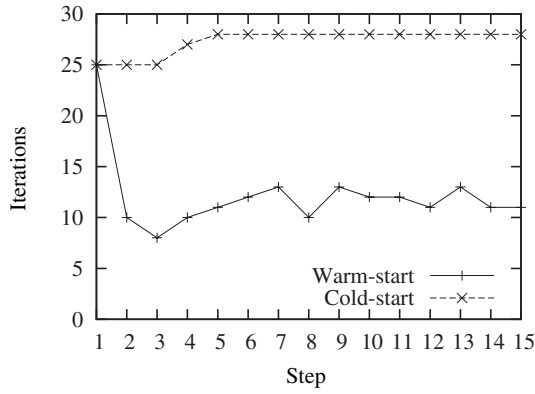


(a) History of prescribed displacement.

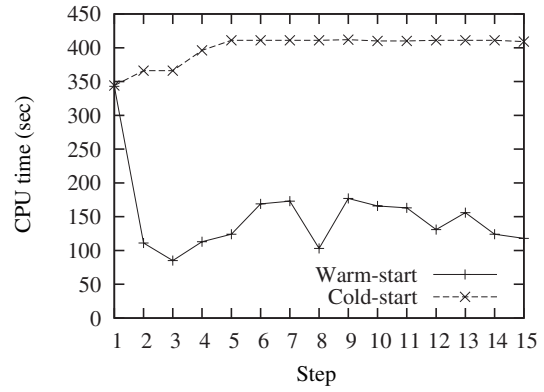


(b) Load-displacement curve.

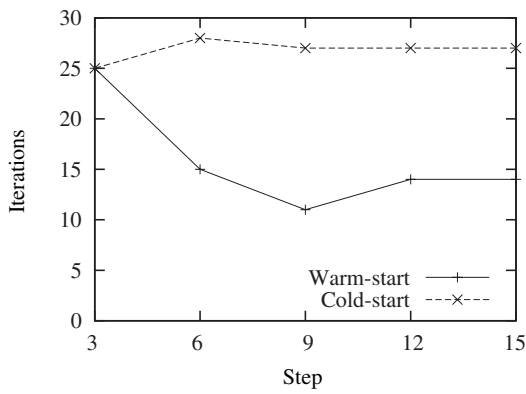
Figure 2: Monotonic loading test of the perforated plate.



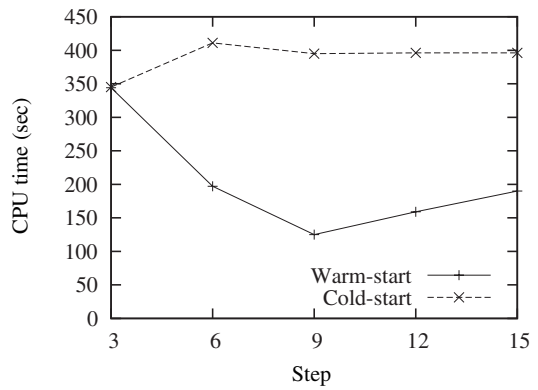
(a) Number of iterations for fine time-discretization.



(b) CPU time for fine time-discretization.



(c) Number of iterations for coarse time-discretization.



(d) CPU time for coarse time-discretization.

Figure 3: Computational results of the monotonic extension of the perforated plate.

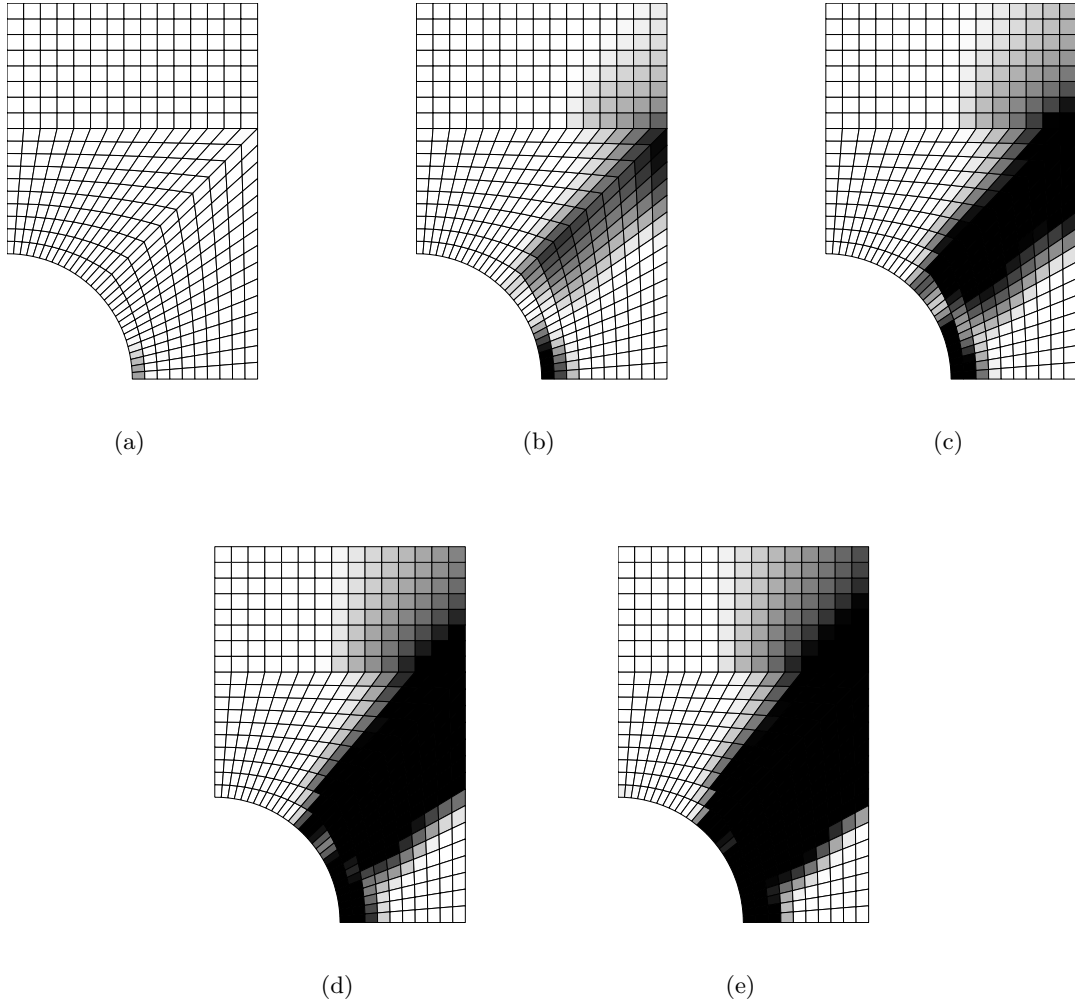


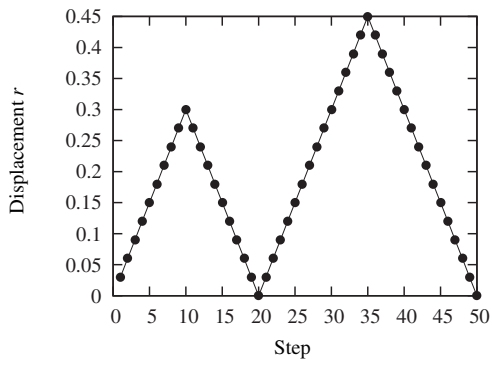
Figure 4: Yield zone evolution of the perforated plate in the monotonic loading test. (a): 4th step; (b): 6th step; (c): 8th step; (c): 10th step; (e): 12th step.

$\bar{u}_{\text{upper}} = r\ell/100$, where the parameter r is increased monotonically as shown in Figure 8(a).

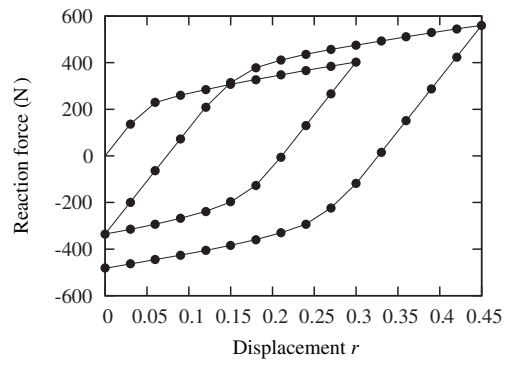
The relation between the displacement and the reaction force is shown in Figure 8(b). Figure 9 shows the number of iterations and CPU time required at each loading step. It is observed that the decrease of computational effort due to our warm-start strategy is about 65% in average. Figure 10 depicts the evolution of the plastic zone during the last four loading steps.

7 Conclusion

We have proposed a methodology with the guaranteed convergence for quasistatic analysis of elastoplastic structures in small deformation. The solution method is based on the polynomial-time primal-dual interior-point method for the second-order cone program (SOCP). The von Mises yield criterion, in conjunction with a combination of linear isotropic and kinematic hardening rules, is considered, which is shown to be formulated as the second-order cone complementarity (SOCC) conditions. Based on the SOCC conditions, the minimization problems of the potential

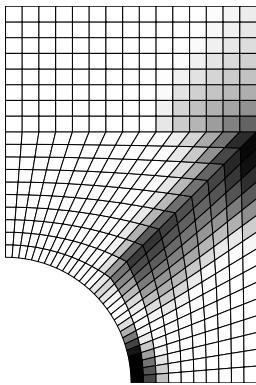


(a) History of prescribed displacement.

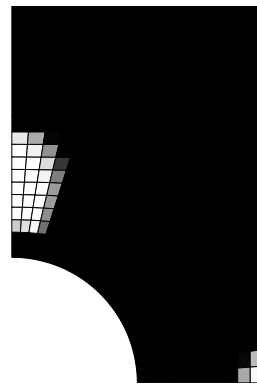


(b) Load-displacement curve.

Figure 5: Cyclic loading test of the perforated plate.



(a)



(b)

Figure 6: Yield zone evolution of the perforated plate in the cyclic loading test. (a): 2nd step; (b): 50th step.

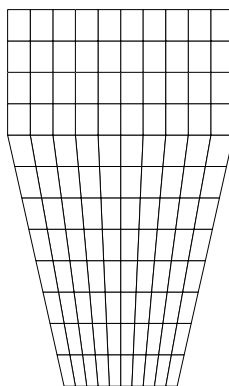
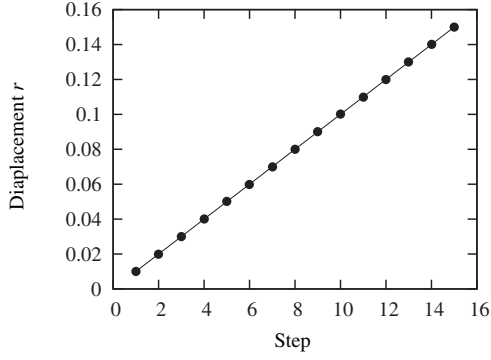
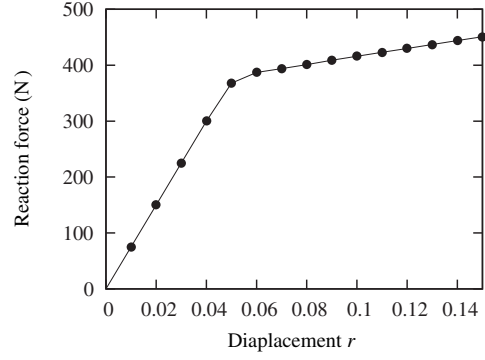


Figure 7: Cross-section of the tapered cylinder.

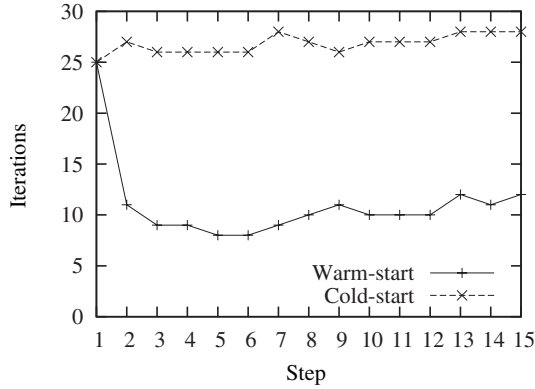


(a) History of prescribed displacement.

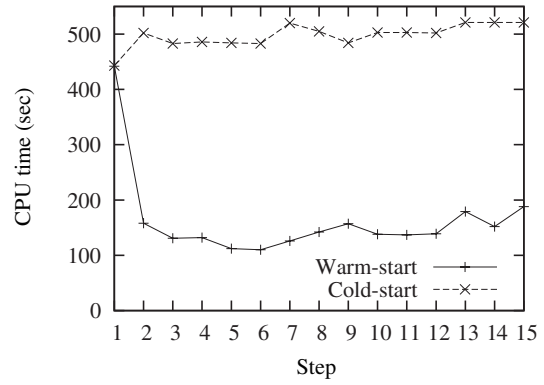


(b) Load-displacement curve.

Figure 8: Extension of the tapered cylinder.



(a) Number of iterations.



(b) CPU time.

Figure 9: Computational results of the extension of the tapered cylinder.

energy and the complementary energy have been formulated as the primal-dual pair of SOCP problems, which are to be solved by using the primal-dual interior-point method. To enhance the numerical performance, we have proposed the warm-start strategy for the interior-point method, which makes use of the incremental solution obtained at the previous loading step in the course of the path-tracing equilibrium analysis to reduce the computational effort required at the current loading step. As the theoretical advantage over the conventional methods, the proposed method is guaranteed to converge to the equilibrium solution within polynomial time. The number of iterations required, in practice, does not depend on the size of loading step. In the numerical experiments the performance of this warm-start strategy has shown the decrease of around 2/3 in the computational time.

Acknowledgments

This study was supported in part by a Grant-in-Aid for Scientific Research from the Ministry of Education, Culture, Sports, Science and Technology of Japan. The work of the second author

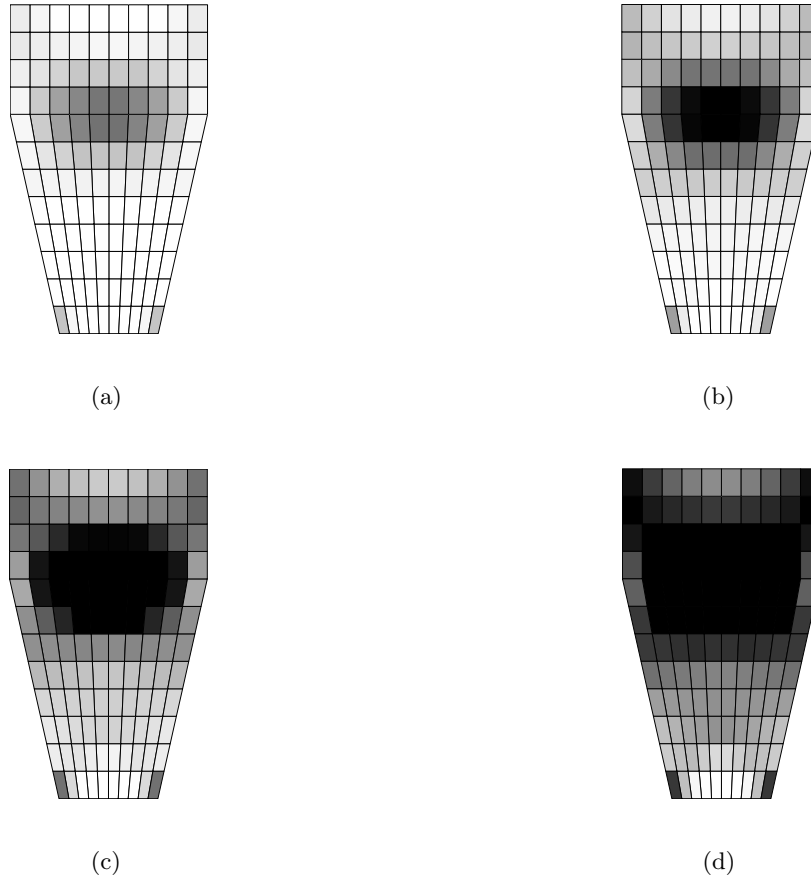


Figure 10: Yield zone evolution of the tapered cylinder. (a): 12th step; (b): 13th step; (c): 14th step; (d): 15th step.

(Y. Kanno) was also supported by Global COE Program “The research and training center for new development in mathematics”.

References

- [1] Alizadeh, F., Goldfarb, D.: Second-order cone programming. *Mathematical Programming*, **95**, 3–51 (2003).
- [2] Benson, H.Y., Shanno, D.F.: An exact primal-dual penalty method approach to warm-starting interior-point methods for linear programming. *Computational Optimization and Applications*, **38**, 371–399 (2007).
- [3] Benson, H.Y., Shanno, D.F.: Interior-point methods for nonconvex nonlinear programming: Regularization and warmstarts. *Computational Optimization and Applications*, **40**, 143–189 (2008).
- [4] Ben-Tal, A., Nemirovski, A.: *Lectures on Modern Convex Optimization: Analysis, Algorithms, and Engineering Applications*. SIAM, Philadelphia (2001).

- [5] Bićanić, N., Pearce, C.J.: Computational aspects of a softening plasticity model for plain concrete. *Mechanics of Cohesive-Frictional Materials*, **1**, 75–94 (1996).
- [6] Bisbos, C.D., Pardalos, P.M.: Second-order cone and semidefinite representations of material failure criteria. *Journal of Optimization Theory and Applications*, **134**, 275–301 (2007).
- [7] Blaheta, R.: Convergence of Newton-type methods in incremental return mapping analysis of elasto-plastic problems. *Computer Methods in Applied Mechanics and Engineering*, **147**, 167–185 (1997).
- [8] Caddemi, S., Martin, J.B.: Convergence of the Newton-Raphson algorithm in elastoplastic incremental analysis. *International Journal for Numerical Methods in Engineering*, **31**, 177–191 (1991).
- [9] Capurso, M., Maier, G.: Incremental elastoplastic analysis and quadratic optimization. *Mechanica*, **5**, 107–116 (1970).
- [10] Contrafatto, L., Ventura, G.: Numerical analysis of augmented Lagrangian algorithm in complementary elastoplasticity. *International Journal for Numerical Methods in Engineering*, **60**, 2263–2287 (2004).
- [11] Cuomo, M., Contrafatto, L.: Stress rate formulation for elastoplastic models with internal variables based on augmented Lagrangian regularization. *International Journal of Solids and Structures*, **37**, 3935–3964 (2000).
- [12] Forsgren A.: On warm starts for interior methods. In: Ceragioli, F., Dontchev, A., Furuta, H., Marti, K., Pandolfi, L. (eds.), *System Modeling and Optimization*. pp. 51–66. Springer, Boston (2006).
- [13] Gondzio, J.: Warm start of the primal-dual method applied in the cutting-plane scheme. *Mathematical Programming*, **83**, 125–143 (1998).
- [14] Han, W., Reddy, B.D.: *Plasticity*. Springer-Verlag, New York (1999).
- [15] Hayashi, S., Yamashita, N., Fukushima, M.: A combined smoothing and regularization method for monotone second-order cone complementarity problems. *SIAM Journal on Optimization*, **15**, 593–615 (2005).
- [16] Hjjaj, M., Fortin, J., de Saxcé, G.: A complete stress update algorithm for the non-associated Drucker–Prager model including treatment of the apex. *International Journal of Engineering Science*, **41**, 1109–1143 (2003).
- [17] Hu, Z.Q., Soh, A.-K., Chen, W.J., Li, X.W., Lin, G.: Non-smooth nonlinear equations methods for solving 3D elastoplastic frictional contact problems. *Computational Mechanics*, **39**, 849–858 (2007).
- [18] Huang, J., Griffiths, D.V.: Observations on return mapping algorithms for piecewise linear yield criteria. *International Journal of Geomechanics*, **8**, 253–265 (2008).

- [19] John, E., Yildırım, E.A.: Implementation of warm-start strategies in interior-point methods for linear programming in fixed dimension. *Computational Optimization and Applications*, **41**, 151–183 (2008).
- [20] Kanno, Y., Martins, J.A.C., Pinto da Costa, A.: Three-dimensional quasi-static frictional contact by using second-order cone linear complementarity problem. *International Journal for Numerical Methods in Engineering*, **65**, 62–83 (2006).
- [21] Krabbenhøft, K., Lyamin, A.V., Sloan, S.W.: Formulation and solution of some plasticity problems as conic programs. *International Journal of Solids and Structures*, **44**, 1533–1549 (2007).
- [22] Krabbenhøft, K., Lyamin, A.V., Sloan, S.W.: Three-dimensional Mohr–Coulomb limit analysis using semidefinite programming. *Communications in Numerical Methods in Engineering*, **24**, 1107–1119 (2008).
- [23] Krabbenhøft, K., Lyamin, A.V., Sloan, S.W., Wriggers, P.: An interior point algorithm for elastoplasticity. *International Journal for Numerical Methods in Engineering*, **69**, 592–626 (2007).
- [24] Liew, K.M., Wu, Y.C., Zou, G.P., Ng, T.Y.: Elasto-plasticity revisited: numerical analysis via reproducing kernel particle method and parametric quadratic programming. *International Journal for Numerical Methods in Engineering*, **55**, 669–683 (2000).
- [25] Maier, G.: A quadratic programming approach for certain classes of non-linear structural problems. *Meccanica*, **3**, 121–130 (1968).
- [26] Maier, G.: Complementary plastic work theorems in piecewise-linear elastoplasticity. *International Journal of Solids and Structures*, **5**, 261–270 (1969).
- [27] Mitchell, J.E.: Restarting after branching in the SDP approach to MAX-CUT and similar combinatorial optimization problem. *Journal of Combinatorial Optimization*, **5**, 151–166 (2001).
- [28] Oñate, E.: *Structural Analysis with the Finite Element Method. Linear Statics. Volume 1: Basis and Solids*. Springer-Verlag (2009).
- [29] Ortiz, M., Popov, E.P.: Accuracy and stability of integration algorithm for elastoplastic constitutive relations. *International Journal for Numerical Methods in Engineering*, **21**, 1561–1576 (1985).
- [30] Pérez-Foguet, A., Rodríguez-Ferran, A., Huerta, A.: Consistent tangent matrices for substepping schemes. *Computer Methods in Applied Mechanics and Engineering*, **190**, 4627–4647 (2001).
- [31] Simo, J.C., Hughes, T.J.R.: *Computational Inelasticity*. Springer-Verlag, New York (1998).

- [32] Simo, J.C., Kennedy, J.G., Taylor, R.L.: Complementary mixed finite element formulations for elastoplasticity. *Computer Methods in Applied Mechanics and Engineering*, **74**, 177–206 (1989).
- [33] Simo, J.C., Taylor, R.L.: Consistent tangent operators for rate-independent elastoplasticity. *Computer Methods in Applied Mechanics and Engineering*, **49**, 221–245 (1985).
- [34] Simo, J.C., Taylor, R.L.: A return mapping algorithm for plane stress elastoplasticity. *International Journal for Numerical Methods in Engineering*, **22**, 649–670 (1986).
- [35] The MathWorks, Inc.: *Using MATLAB*. The MathWorks, Inc., Natick (2009).
- [36] Tin-Loi, F., Pang, J.S.: Elastoplastic analysis of structures with nonlinear hardening: A nonlinear complementarity approach. *Computer Methods in Applied Mechanics and Engineering*, **107**, 299–312 (1993).
- [37] Tin-Loi, F., Xia, S.H.: Nonholonomic elastoplastic analysis involving unilateral frictionless contact as a mixed complementarity problem. *Computer Methods in Applied Mechanics and Engineering*, **190**, 4551–4568 (2001).
- [38] Tu, X., Andrade, J.E., Chen, Q.: Return mapping for nonsmooth and multiscale elastoplasticity. *Computer Methods in Applied Mechanics and Engineering*, **198**, 2286–2296 (2009).
- [39] Tütüncü, R.H., Toh, K.C., Todd, M.J.: Solving semidefinite-quadratic-linear programs using SDPT3. *Mathematical Programming*, **B95**, 189–217 (2003).
- [40] Xia, Y: A Newton’s method for perturbed second-order cone programs. *Computational Optimization and Applications*, **37**, 371–408 (2007).
- [41] Yamashita, M., Fujisawa, K., Kojima, M.: Implementation and evaluation of SDPA6.0 (SemiDefinite Programming Algorithm 6.0). *Optimization Methods and Software*, **18**, 491–505 (2003).
- [42] Zhang, H.W., He, S.Y., Li, X.S., Wriggers, P.: A new algorithm for numerical solution of 3D elastoplastic contact problems with orthotropic friction law. *Computational Mechanics*, **34**, 1–14 (2004).
- [43] Zhang, H.W., Zhong, W.X., Wu, C.H., Liao, A.H.: Some advances and applications in quadratic programming method for numerical modeling of elastoplastic contact problems. *International Journal of Mechanical Science*, **48**, 176–189 (2006).
- [44] Zhong, W., Sun, S.: A finite element method for elasto-plastic structures and contact problems by parametric quadratic programming. *International Journal for Numerical Methods in Engineering*, **26**, 2723–2738 (1988).
- [45] Zhu, C.: A finite element-mathematical programming method for elastoplastic contact problems with friction. *Finite Elements in Analysis and Design*, **20**, 273–282 (1995).

A Proof of Proposition 4

Proof. Suppose that (32)–(34) are satisfied. It follows from Proposition 2 that one of the following cases becomes true:

$$\begin{aligned} \text{Case 1 : } & \sqrt{\frac{2}{3}}s_K = 0, \dot{\boldsymbol{\beta}} = \mathbf{o}, \quad \gamma \geq \|-\dot{\boldsymbol{\epsilon}}_p\|; \\ \text{Case 2 : } & \sqrt{\frac{2}{3}}s_K \geq \|\dot{\boldsymbol{\beta}}\|, \quad \gamma = 0, \dot{\boldsymbol{\epsilon}}_p = \mathbf{o}; \\ \text{Case 3 : } & \sqrt{\frac{2}{3}}s_K = \|\dot{\boldsymbol{\beta}}\|, \quad \gamma = \|-\dot{\boldsymbol{\epsilon}}_p\|, \quad -\dot{\boldsymbol{\epsilon}}_p = -\gamma \frac{\dot{\boldsymbol{\beta}}}{\|\dot{\boldsymbol{\beta}}\|}, \end{aligned}$$

where $\sqrt{\frac{2}{3}}s_K\gamma \neq 0$.

It follows from (16) that $s_K = 0$ if and only if $\gamma = 0$. Therefore, in Cases 1 and 2 we have $s_K = \gamma = 0$. Since (32) implies $\dot{\boldsymbol{\beta}} = \mathbf{o}$, we see that (18) is satisfied. In Case 3, the relation between $\dot{\boldsymbol{\epsilon}}_p$ and $\dot{\boldsymbol{\beta}}$ can be reduced to

$$\dot{\boldsymbol{\beta}} = \|\dot{\boldsymbol{\beta}}\| \frac{\dot{\boldsymbol{\epsilon}}_p}{\gamma} = \sqrt{\frac{2}{3}}s_K \frac{\dot{\boldsymbol{\epsilon}}_p}{\gamma}. \quad (55)$$

Substitution of (5) into (55) yields

$$\dot{\boldsymbol{\beta}} = \sqrt{\frac{2}{3}}s_K \frac{\boldsymbol{\eta}}{\|\boldsymbol{\eta}\|}.$$

Thus (18) is satisfied.

Conversely, suppose that (18) holds. We easily see that (18) implies $\|\dot{\boldsymbol{\beta}}\| = \sqrt{\frac{2}{3}}s_K$, and hence (32) is satisfied. Similarly, (5) implies $\|\dot{\boldsymbol{\epsilon}}_p\| = \gamma$, and hence (33) is satisfied. Finally, by substituting (18) and (5), the left-hand side of (34) is reduced to

$$\begin{aligned} \sqrt{\frac{2}{3}}s_K\gamma - \dot{\boldsymbol{\beta}} : \dot{\boldsymbol{\epsilon}}_p &= \sqrt{\frac{2}{3}}s_K\gamma - \left(\sqrt{\frac{2}{3}}s_K \frac{\boldsymbol{\eta}}{\|\boldsymbol{\eta}\|} \right) : \left(\gamma \frac{\boldsymbol{\eta}}{\|\boldsymbol{\eta}\|} \right) \\ &= \sqrt{\frac{2}{3}}s_K\gamma - \sqrt{\frac{2}{3}}s_K\gamma \frac{\boldsymbol{\eta} : \boldsymbol{\eta}}{\|\boldsymbol{\eta}\|^2} \\ &= 0, \end{aligned}$$

and hence (34) is satisfied. Consequently, (18) implies (32)–(34), which concludes the proof. \square